SAPIENZA
UNIVERSITÀ DI ROMA

DOTTORATO DI RICERCA IN BIOCHIMICA
CICLO XXIII (A.A. 2007-2010)

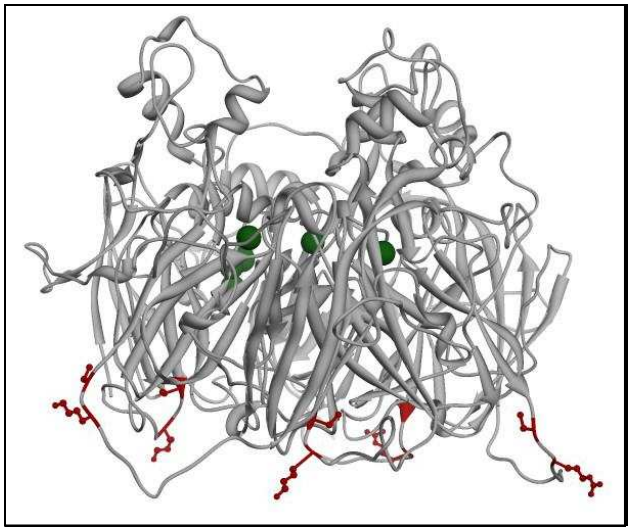

Structural and functional mechanisms of Aceruloplasminemia

Docente guida
Prof.
Donatella Barra

Coordinatore
Prof.
Paolo Sarti

Dottorando
Giovanni De Francesco

TABLE OF CONTENTS

INTRODUCTION

IRON HOMEOSTASIS IN HUMANS

The management of iron is a critical issue for all living cells, where its presence is necessary to carry out numerous vital biological reactions, but because of its highly reactive nature, iron is extremely toxic if its intracellular concentrations are not tightly regulated.

The divalent state of iron makes it highly toxic, as it can rapidly react with hydrogen peroxide and molecular oxygen to produce free radicals. Free radical formation can promote lipid peroxidation, DNA strand breaks, and modification or degradation of biomolecules, eventually leading to cell death. Cells have therefore evolved a sophisticated mechanism consisting of an array of proteins that regulate the amount of free iron in cells by modulating its uptake, storage, and export. Together, these proteins provide a state of cellular equilibrium whereby iron is readily available for all metabolic functions but sheltered from taking part in cytotoxic reactive oxygen species (ROS)-generating reactions.

Dietary iron absorption requires that iron traverse both the apical and basolateral membranes of absorptive epithelial cells in the duodenum to reach the blood, where it is incorporated into transferrin. The transport of non-heme iron across the apical membrane occurs via the divalent metal transporter 1 (DMT1), the only known intestinal iron importer.

Dietary non-heme iron exists mainly in ferric form (Fe^{3+}) and must be reduced prior to transport. Duodenal cytochrome B (DcytB) is a reductase localized in the apical membrane of intestinal enterocytes and is a major, but most likely not the only, reductase. In parallel, iron is also absorbed as heme.

Cytosolic iron in intestinal enterocytes can be either stored in ferritin or exported into plasma by the basolateral iron exporter ferroportin (Fpn). Fpn is most likely the only cellular iron exporter in the duodenal mucosa as well as in macrophages, hepatocytes and the syncytial trophoblasts of the placenta. The export of iron by Fpn depends on two multicopper oxidases, ceruloplasmin (Cp) in the circulation and hephaestin on the basolateral membrane of enterocytes, which convert Fe^{2+} to Fe^{3+} for incorporation of iron into transferrin.

Intestinal iron absorption is tightly controlled and is dependent on body

iron needs. Recent studies indicate that this process is accomplished by modulating the expression levels of DMT1, DcytB and ferroportin by multiple pathways.

IRON TRAFFICKING INSIDE THE BRAIN

Iron is essential for a plethora of functions in all cells. In the brain these include neurotransmission, myelination and cell division.

In the circulation, iron is bound to transferrin; the hydrophilic nature of the iron-containing transferrin prevents its passage into the brain, but to circumvent this feature and simultaneously nourish neurons and glial cells, the brain, as the only organ in the body with this capacity, expresses receptors for transferrin (transferrin receptor 1) on the luminal side of its capillaries (Angelova-Gateva, 1980; Jefferies et al., 1984; Kawabata et al., 1999). Hence, transferrin receptor-mediated uptake of iron by brain capillary endothelial cells (BCECs) followed by further transport into the brain is the major mechanism by which iron is transported into the brain.

Blood to brain transport of iron

Blood to endothelium transport

Several observations indicate that transferrin receptors are essential for iron uptake by the brain. In embryonic life, transferrin receptors are expressed by proliferating neural progenitor cells (Copp et al., 1992) and BCECs from the time they appear (Moos et al., 1998).

Failure of transferrin receptor expression in fetal mice results in lethal outcomes during development with severe defects in the CNS, most probably because the lack of transferrin receptors prevents iron uptake by dividing brain cells (Levy et al., 1999).

The transferrin receptor is continuously expressed by BCECs and neurons in the developing rodent brain (Moos et al. 1998), but the expression pattern is age-dependent with peak expression in BCECs around the second postnatal week. In neurons expression reaches its highest levels from the beginning of the fourth postnatal week, when the blood-brain barrier (BBB) integrity is fully developed and the rate of iron transport into the brain is lower than that of the developing brain (Taylor and Morgan, 1990).

Endothelium to brain transport

Binding of iron-transferrin to the transferrin receptor is followed by docking and formation of an endosome that enters the BCEC. The endosomal pH is slightly acidic, which causes the iron to be liberated from transferrin. As described in many other cell types, the presence of DMT1 allows the transport of divalent cations out of the endosome and into the cytosol while exchanging the cationic load inside the endosome with two protons (Gunshin et al., 1997).

Surprisingly DMT1 could not be detected in BCECs in a series of independent investigations using a panel of antibodies raised against different regions of the DMT1 molecule such as the conserved trans-membrane region and the variable C-terminal region with or without an iron responsive element (+IRE vs. -IRE) (Moos and Morgan, 2004; Moos and Rosengren Nielsen, 2006). In contrast, DMT1 was readily detectable in neurons where it was present in a punctate form in the cytoplasm and choroid plexus epithelial cells.

Based on these observations it should be possible that DMT1 is unlikely to play a role for iron-transport across BCECs, and that iron is transported from the luminal to the abluminal surface of these cells inside vesicles without any step which leads to its release from the endosome into the cytosol and from there into the brain interstitium.

If transferrin receptor-containing vesicles are transported through the BCECs and fuse with the abluminal side, they would offer iron detached from transferrin and ready to be transported further into the brain. The iron atoms would probably be in their ferric form, and the process would not require the function of ferroportin, which is responsible for ferrying iron out of other types of cells (Wessling-Resnick, 2006). There is disagreement as to whether ferroportin is present in (Wu et al., 2004) or absent from BCECs (Moos and Rosengren Nielsen, 2006).

Iron release from transferrin on the abluminal surface of BCECs.

BCECs cells are intimately connected with astrocytes. Astrocytic end-feet form intimate contacts with the abluminal side of BCECs of around 95% of the area denoted by the basal lamina.

The astrocytic end-feet processes could play an important metabolic role for neutralization of solutes transported through the BCECs into the brain to preclude the risks of such solutes impairing the delicate extracellular environment of the brain. In the case of iron, astrocytes could be important

regulators of iron import into the brain as proposed in recent publications (Moos and Morgan, 2004; Moos and Rosengren Nielsen, 2006).

Subsequent to the binding of iron-transferrin at the luminal surface of the BCEC, the transferrin-receptor complex is internalized in an endosome that is transported toward the abluminal side of the BCEC. The acidic environment of the endosomes leads to release of iron from transferrin. After fusing with the abluminal side, the content of the endosome is released, and iron binds to either apo-transferrin present in the brain interstitium or low-molecular weight substances like ATP and citrate. Astrocytes probably also take up iron bound to ATP or citrate. The endosome containing the apo-transferrin recycles to the luminal cell surface where it is released from the transferrin receptor and returns to blood plasma (Moos et al., 2007).

Circulation of iron inside the brain interstitium

Provided molecules released by astrocytes capture iron transported through BCECs, the interstitium will contain non-transferrin bound iron complexed to smaller organic molecules like citrate, ATP and ascorbic acid (c.f. Bradbury, 1997). The BCECs are likely to release ferric iron, whereas ferrous iron release is likely to occur by secretion from neurons and oligodendrocytes because of their expression of the iron exporter ferroportin (Burdo et al., 2001; Wu et al., 2004; Moos and Rosengren Nielsen, 2006), although the oxidation state of iron transported by ferroportin is not yet firmly established.

Beside from circulating in the brain interstitium bound to low-molecular weight constituents like ATP and citrate, ferric iron is thought to be mainly bound to transferrin. The most likely source for transferrin in the brain interstitium derives from diffusion from the ventricles.

Another protein with potential to act as an extracellular iron carrier in the brain is lactoferrin (a.k.a. lactotransferrin). It is structurally closely related to transferrin but has an even higher affinity for ferric iron (Morgan, 1981; Brock, 1995). It is known to be synthesized in the mammary glands and neutrophil polymorphonuclear leukocytes and to circulate in low concentrations in blood plasma. It is not believed to play a significant role in the plasma transport of iron but, rather, to be involved in inflammatory reactions, at least in part because of anti-bacterial properties. Lactoferrin is present in CSF, in increased concentrations after cerebral bleeding or infarction (Terent et al., 1981). A lactoferrin receptor is present on brain microvessels, and there is evidence from in vitro studies that lactoferrin can traverse BCECs (Fillebeen et al., 1999).

Hence, brain lactoferrin may be derived from the blood, although local synthesis probably also occurs (Siebert and Huang, 1997). Lactoferrin and its receptor have been detected in neurons and glial cells in many different neurodegenerative diseases (Leveugle et al., 1994; Faucheux et al., 1995). It is likely that, in the brain, lactoferrin acts as a scavenger for iron released from degenerating and damaged cells thereby reducing the potentially toxic effects of such iron. However, it should be noted that there is no evidence that it functions as a quantitatively significant transporter of iron under normal conditions.

Iron uptake and export by neuronal cells

Neurons take up iron-transferrin injected into the brain (Moos and Morgan, 1998b), and they contain both transferrin receptors and DMT1, which clearly indicates that they can take up iron-transferrin and transport it to endosomes from where iron is pumped into the cytoplasm.

The neurons probably also take up non-transferrin bound iron present in the brain interstitium, as they take up iron-citrate in culture conditions (Moos et al., 2007).

Neurons are thought to regulate their iron levels so that iron not used for metabolic purposes is released from the cells. The observation that neuronal ferroportin is virtually ubiquitously expressed in the brain suggests that iron-export mediated by ferroportin is a permanently active mechanism, which ensures iron-homeostasis inside the neuron.

Iron is thought to undergo axonal and dendritic transport, and as ferroportin is found in the somata, axons, and dendrites of neurons, it probably plays an important role to regulate iron levels everywhere in the neuron (Moos and Rosengren Nielsen, 2006). Neurons of some forebrain nuclei, however, also contain ferritin, showing that neurons are capable of storing iron (Hansen et al., 1999).

Macroglia

Astrocytes are considered to play an important role in iron homeostasis of the brain, yet the mechanisms involved in the uptake of iron into astrocytes remain elusive. In the intact brain, astrocytes are devoid of transferrin receptors, suggesting that they take up iron by a mechanism that does not involve the transferrin receptor (Moos and Morgan, 2004). It has been shown in rat astrocyte-rich primary cultures that these cultures express the mRNAs of two membrane-bound ferric reductases, DcytB and SDR2, and reduce extracellular

ferric iron (Tulpule et al., 2010). These data indicate that, in addition to the DMT1-mediated uptake of ferrous iron, astrocytes can accumulate ferric and ferrous iron by mechanisms that are independent of DMT1 or transferrin.

The export of iron from astrocytes is thought to involve the copper-containing protein ceruloplasmin that exhibits ferroxidase activity, which is capable of oxidizing ferrous iron to ferric iron and is present on astrocytes in a membrane-bound form (Patel and David, 1997). Depletion of the ceruloplasmin gene in mice was recently shown to affect astrocytes in that they accumulated iron and showed signs of pathological changes (Jeong and David, 2006). These data confirm the current hypothesis that ceruloplasmin is needed for export of iron from astrocytes (Klomp et al., 1996). Deletion of ceruloplasmin affected some neurons of the cerebellum, and it was suggested that the failure of astrocytes to oxidize ferrous iron could affect the iron availability for the neurons, causing them to become iron-depleted either by reducing the concentration of iron in the brain extracellular space or by impairment of a direct iron-transfer between astrocytes and neurons (Jeong and David, 2006).

FERROPORTIN

Ferroportin (Fpn) is the only known mammalian cellular iron exporter and is present on most cell types that deliver iron into plasma (Ganz and Nemeth, 2006). Expression of Fpn leads to export of iron and a decrease in the cellular iron storage protein ferritin (Nemeth et al., 2004).

Human Fpn is constituted by 571 aminoacids, sequences are now available for Fpn from many vertebrates, including mouse and zebrafish which were the first Fpns identified, and numerous others which can be retrieved from annotated genome projects. The protein is well-conserved, with over 60% identity between distantly related proteins such as human and zebrafish Fpn, and Fpn-like sequences identified in *Arabidopsis thaliana* and *Caenorhabditis elegans*, indicating a wide distribution and a critical role for Fpn.

The topology of Fpn was initially predicted to vary between 9 and 12 TM regions with the N-terminus generally positioned inside and the C-terminus intra- or extracellular, depending on the number of TM segments. Experiments from different groups have used recombinant epitope-tagged Fpn to probe the topology of the protein by immunofluorescence (Liu et al., 2005; Rice et al., 2009). Despite initial controversial results, it is now firmly established that both

N- and C-terminal extremities of Fpn are intracellular, and a consensus on a topological model of Fpn with 12 TM has been reached (Figure 1).

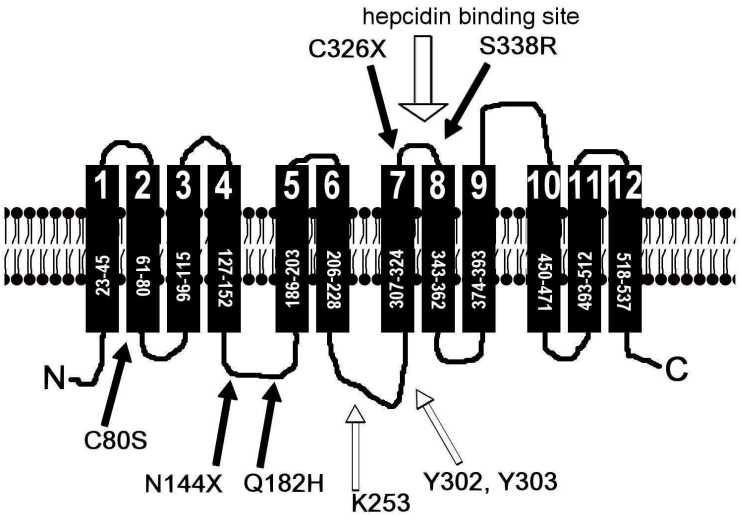

Figure 1. Topology of human ferroportin. White arrows indicate aminoacid residues required for internalization and degradation of Fpn, black arrows indicate mutations causing resistance to hepcidin; the position of the hepcidin-binding site is also shown.

Different models generally agree over position of TM 2-4 and 9-12, while TM 1 and TM 5-8 are less well-defined. Structural features relevant for Fpn function are a large intracellular loop between TM 6 and 7, which contains key residues important for internalization and degradation of Fpn, and an extracellular loop between TM 7 and 8, where the hepcidin-binding site is located.

Fpn is regulated by several mechanisms, but particularly through its interaction with hepcidin, a peptide produced by the liver in response to iron stores, erythropoiesis, hypoxia and inflammation. Hepcidin binds to Fpn and does not inhibit transport activity directly, but rather induces the internalization of Fpn from cell surfaces (Nemeth et al., 2004) (Figure 2). Once internalized, Fpn is degraded in the lysosome.

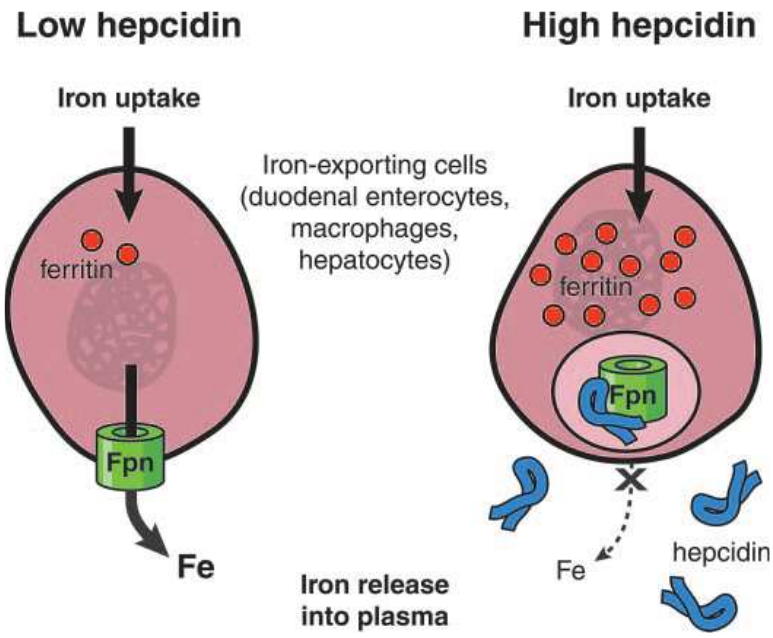

Figure 2. Hepcidin regulates cellular iron export into plasma. When hepcidin concentrations are low, ferroportin (Fpn) molecules are displayed on the plasma membrane and export iron. When hepcidin concentrations increase, hepcidin binds to ferroportin molecules and induces their internalization and degradation, and iron release is decreased progressively. Illustration by Josh Gramling—Gramling Medical Illustration.

Most hereditary iron overload diseases can be explained by inadequate production of hepcidin in response to iron stores or by mutations in Fpn (Pietrangelo, 2006). Thus, the presence of cell surface Fpn may be the critical determinant in mammalian iron homeostasis.

Hepcidin is a 25-aminoacid peptide hormone secreted by hepatocytes, circulating in blood plasma and excreted in urine (Park et al., 2001). It is structurally similar to cysteine-rich, cationic antimicrobial peptides of the defensin family and it possesses a -hairpin structure stabilized by four disulphide bonds (Ganz and Nemeth, 2006) (Figure 3). Hepcidin plays an essential role in maintaining iron homeostasis, and the dysregulation of its production underlies many iron disorders. Increased expression of hepcidin as a

result of inflammatory mediators causes iron-restricted anemia (Roy et al., 2007), whereas hepcidin deficiency results in iron overload with iron deposition in the liver and other parenchyma (Roetto et al., 2003). Hepcidin acts by regulating the cellular concentration of its receptor, ferroportin.

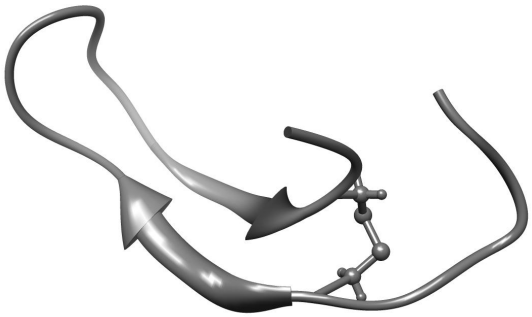

Figure 3. Structure of hepcidin. The connectivity of the 8 cysteines has been recently revised. Only the disulphide bond connecting C1-C8 is shown because it is essential for hepcidin biological activity.

The molecular mechanisms of hepcidin-dependent degradation of Fpn have been elucidated and the hepcidin-binding site has been recently identified (De Domenico et al., 2007, 2008, 2009). Proteins targeted for degradation are usually modified by ubiquitination and/or phosphorylation, and Fpn is no exception to this rule. The first event following binding of hepcidin, is phosphorylation of Fpn on one of two adjacent tyrosine residues, Tyr-302 and Tyr-303, that takes place at the plasma membrane (De Domenico et al., 2007). Ubiquitination at Lys-253 occurs once Fpn is internalized in a dynamin-dependent process requiring clathrin-coated pits. The two tyrosines and the lysine residues modified to signal internalization and degradation of Fpn are located in a large intracellular loop between TM 6 and 7 (see Figure 1), suggesting that phosphorylation might induce structural alterations which trigger ubiquitination.

The hepcidin-binding site on Fpn has been identified in a conserved extracellular loop between aminoacids 324-343 (De Domenico et al., 2008). It is interesting to note that this loop follows TM 7 and is in close proximity to the cytosolic loop containing Tyr-302 and Tyr-303, and Lys-253 (see Figure 1). It has been suggested that hepcidin binding to Fpn could cause small changes in protein conformation that might lead to a change in the conformation of the

cytosolic loop making the tyrosines accessible for phosphorylation. Analysis of the sequence surrounding Tyr-302 and Tyr-303 suggested that it could be a potential src kinase phosphorylation site. Recent data have identified Jak2 as the kinase responsible for hepcidin-induced phosphorylation of Fpn (De Domenico et al., 2009).

The species of iron transported by Fpn is thought to be Fe^{2+}, which is converted to Fe^{3+} by the multicopper oxidases, ceruloplasmin or hephaestin, which function as ferroxidases. A new mechanism of ferroportin regulation has been recently discovered that requires the ferroxidase activity of ceruloplasmin: lack of oxidase-active ceruloplasmin leads to internalization and degradation of ferroportin (De Domenico et al., 2007). The ferroxidase activity of ceruloplasmin appears to be responsible for generating an iron gradient, leading to the loss of Fpn-bound iron (Figure 4). In the absence of Cp, iron bound to Fpn results in Fpn internalization.

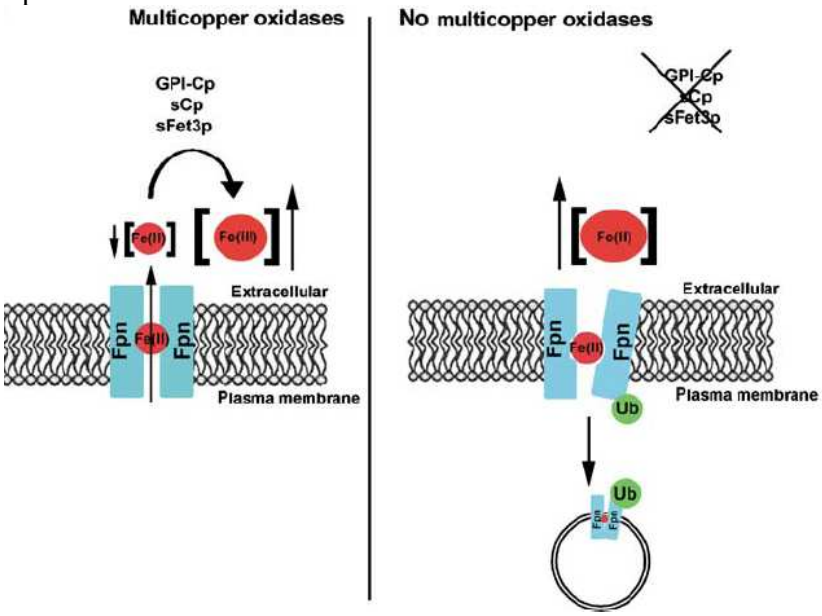

Figure 4. Model for the role of Cp in the cell surface localization of Fpn. Fpn transports Fe(II) from the cytosol across the plasma membrane. Multicopper oxidases ensure low extracellular Fe(II) concentrations by catalyzing the oxidation of Fe(II) to Fe(III). In the absence of Cp, iron may remain in the Fpn channel, affecting Fpn conformation and resulting in Fpn ubiquitination, which leads to Fpn internalization and degradation.

The absence of either multicopper oxidase results in decreased plasma iron and increased iron retention in normally iron exporting cells. The removal of Fpn from the cell surface completes a homeostatic loop in which iron transport is coordinated with iron need.

CERULOPLASMIN

Ceruloplasmin (Cp) was first isolated from plasma and characterized as a copper-containing protein by Holmberg and Laurell in 1948 (Holmberg and Laurell, 1948). Soon thereafter Scheinberg and Gitlin demonstrated a marked decrease in the concentration of this protein in serum samples from patients with Wilson disease, providing a biochemical test for this disorder that is still in clinical use today (Scheinberg and Gitlin, 1952). Frieden (Osaki et al., 1966) demonstrated that ceruloplasmin is a ferroxidase, and this observation, taken together with Cartwright's (Lee et al., 1968) detailed nutritional studies in copper-deficient pigs, suggested a role for ceruloplasmin in iron homeostasis. In 1984 the complete amino acid sequence of human ceruloplasmin was determined, revealing the single-chain structure of this molecule (Takahashi et al., 1994). Solution of the crystal structure of ascorbate oxidase permitted sequence alignment and delineation of the copper-binding amino acids in ceruloplasmin (Messerschmidt et al., 1989). Isolation and characterization of ceruloplasmin cDNA clones confirmed the amino acid sequence obtained by protein chemistry and demonstrated abundant expression of the ceruloplasmin gene in the liver (Koshinsky et al., 1986, Yang et al., 1986). An essential role for ceruloplasmin in iron metabolism was established in 1995 with the identification of patients with aceruloplasminemia (Harris et al., 1995, Yoshida et al., 1995).

MULTICOPPER OXIDASES

Ceruloplasmin is a member of the multicopper oxidase family of enzymes. This evolutionarily conserved group of proteins is characterized by the presence of three types of spectroscopically distinct copper sites (Solomon et al., 1996). Ceruloplasmin contains three type 1 copper sites, and charge transfer between the cysteine ligand sulfur and the copper at these sites results in strong absorption at 600 nm, conferring an intense blue color to this protein. A single type 2 copper is in close proximity to two antiferromagnetically coupled type 3 copper ions that absorb at 330 nm. The type 2 and type 3 coppers form a

trinuclear copper cluster that is the site of oxygen binding and reduction during the catalytic cycle (Calabrese et al., 1989). Resolution of the structure of human ceruloplasmin by X-ray crystallography has confirmed the presence of this trinuclear cluster as well as the identity of each of the amino acid copper ligands (Zaitseva et al., 1996).

Multicopper oxidases utilize the facile electron chemistry of bound copper ions to couple substrate oxidation with the four-electron reduction of dioxygen to water. Electrons pass from the substrate to the type 1 copper and then to the trinuclear copper cluster and subsequently to the oxygen molecule bound at this site (Solomon et al., 1996).

Whereas the signature sequences encompassing the amino acid ligands for copper are highly conserved amongst all multicopper oxidases, the substrates, the number of type 1 coppers and precise mechanisms of intramolecular electron transfer vary from protein to protein (Machonkin et al., 2001). Unique members of this family of enzymes, which include the well-characterized proteins laccase and ascorbate oxidase, are present in bacteria, fungi, yeast, plants, worms, parasites, and mammals.

Known substrates of the multicopper oxidases include manganese, iron, nitrate, bilirubin, phenols, and ascorbate. In addition to ceruloplasmin, several multicopper oxidases have been identified as playing a critical role in iron homeostasis. Fet3 is a ferroxidase essential for iron uptake in yeast, and hephaestin is a ceruloplasmin homologue that is required for efficient iron efflux from the placenta and enterocytes in mammals (Askwith et al., 1994, Vulpe et al., 1999).

CERULOPLASMIN X-RAY STRUCTURE

The three-dimensional molecular structure of human serum ceruloplasmin has been reinvestigated using X-ray synchrotron data collected at 100 K from a crystal frozen to liquid nitrogen temperature (Bento et al., 2007). The resulting model, with an increase in resolution from 3.1 to 2.8 Å compared to the first structure, which was solved in 1996 (Zaitseva et al., 1996), gives an overall improvement of the molecular structure, in particular the side chains.

OVERALL ORGANIZATION OF THE MOLECULE

Fig. 5 shows the overall organization of the human ceruloplasmin (hCP) molecule and the locations of various metal cations: Cu^{2+}, Ca^{2+} and Na^{+}. The molecule is comprised of six cupredoxin-type domains coloured red through to

purple. Domains 1, 3 and 5 comprise some 190 amino-acid residues, whereas the even domains are smaller, with around 150 residues. Domains 2, 4 and 6 possess a binding site for a mononuclear type 1 copper centre; the trinuclear copper centre comprising a type 2 copper ion and two type 3 copper ions is located between domains 1 and 6. The lower surface of the molecule is relatively planar, with the exception of the loops connecting the domains, but the top surface has three large protuberances formed by loops from pairs of odd and even domains. Thus, the loop between β-strands 1 and 2 of an odd domain packs against the loop between β-strands 1 and 2 of an even domain and this association is assisted by a Na^{+} cation. The Ca^{2+} cation is located in domain 1 in a configuration very similar to that found in the activated bovine factor Va. The Na^{+} sites appear to play a structural role in providing rigidity to the three protuberances on the top surface of the molecule. These features probably help to steer substrates towards the mononuclear copper sites prior to their oxidation and to restrict the size of the approaching substrate.

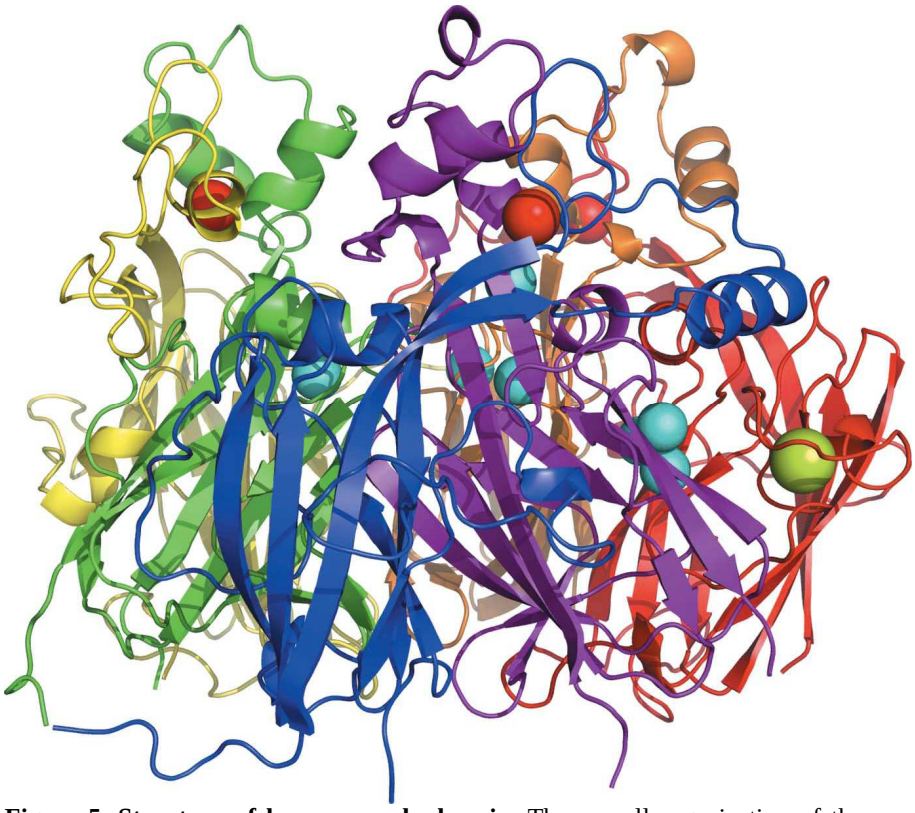

Figure 5. Structure of human ceruloplasmin. The overall organization of the ceruloplasmin molecule, showing the six cupredoxin domains (domains 1, 2, 3, 4, 5 and 6 in red, orange, yellow, green, blue and purple, respectively) and the locations of the metal-binding sites: Cu^{2+} as blue spheres, Ca^{2+} as an olive-green sphere and Na^{+} as red spheres. The relatively planar bottom surface and the protuberances at the top surface are clearly visible. The figure was prepared with PyMOL (DeLano).

THE MONONUCLEAR TYPE 1 COPPER-BINDING SITES

Ceruloplasmin contains three mononuclear type 1 copper-binding sites located in the even domains 2, 4 and 6 (Fig 6). The type 1 sites in domains 4 and 6 are typical blue-copper sites with two histidines and a cysteine ligand at around 2.0 Å and a fourth weaker ligand, a methionine, at distance of around 3.0 Å. The mononuclear site in domain 2 is similar to that found in several fungal laccases (Ducros et al., 2001; Piontek et al., 2002; Garavaglia et al., 2004) in that it lacks the weak methionine ligand, which is replaced by an aliphatic leucine residue at

a closest distance of around 3.5 Å.

Ceruloplasmin is unique among the other multicopper oxidases in that it contains three type 1 ‘integral’ copper ions in the even-numbered domains, whereas only the type 1 copper in domain 6 at a distance of some 12–13 Å from the trinuclear cluster is absolutely necessary for ceruloplasmin to perform catalytic action according to the schemes suggested for ascorbate oxidase and laccase (Messerschmidt et al., 1992; Bento et al., 2005). The distances between the copper ions in the even domains of around 18 Å is well within the range of effective electron transfer (Lindley et al., 1997; Machonkin and Solomon, 2000) and it has been suggested that the copper ions in domains 2 and 4 could provide a slower route of electron transfer, thus permitting the oxidation of more than one substrate molecule at a time. This could in turn accomplish a more effective transfer of four electrons to the dioxygen molecule from the reducing substrate.

The role of the copper ion in domain 2, however, remains intriguing. First, none of the metal-soaking or organic substrate-soaking experiments gave any indication that reducing substrates bind in domain 2. Second, the replacement of the axial ligand of the type 1 copper in domain 2, Leu329, with Met by site-directed mutagenesis resulted in a silent mutation in that it failed to modify either the spectroscopic or catalytic properties of the mutated protein (Bielli et al., 2001). Whether the type 1 site in domain 2 is an ‘evolutionary relic’ and therefore functionally silent or whether this copper ion is destined for other functions still remains unclear.

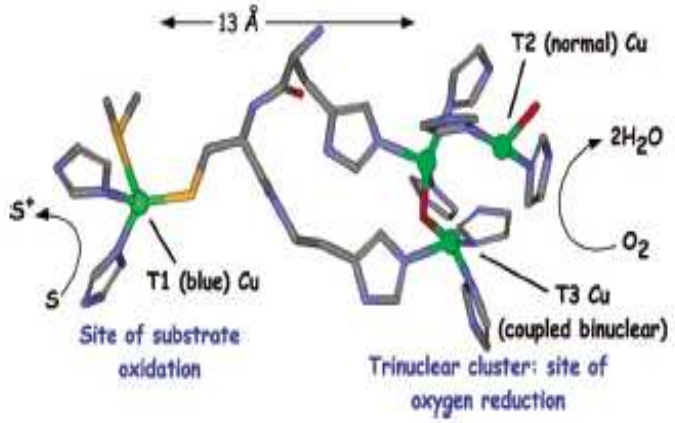

Figure 6. The trinuclear cluster between domains 1 and 6 and the type 1 site in domain 6 are connected by a His-Cys-His sequence motif, where the type 1 copper Cys ligand is flanked by two His ligands to the trinuclear cluster.

THE TRINUCLEAR COPPER CENTRE

The trinuclear copper centre comprising two type 3 copper ions and a type 2 ion may well contain a mixture of states, but the dominant species is that with a diatomic species bound to the trinuclear centre as shown in Fig. 7.

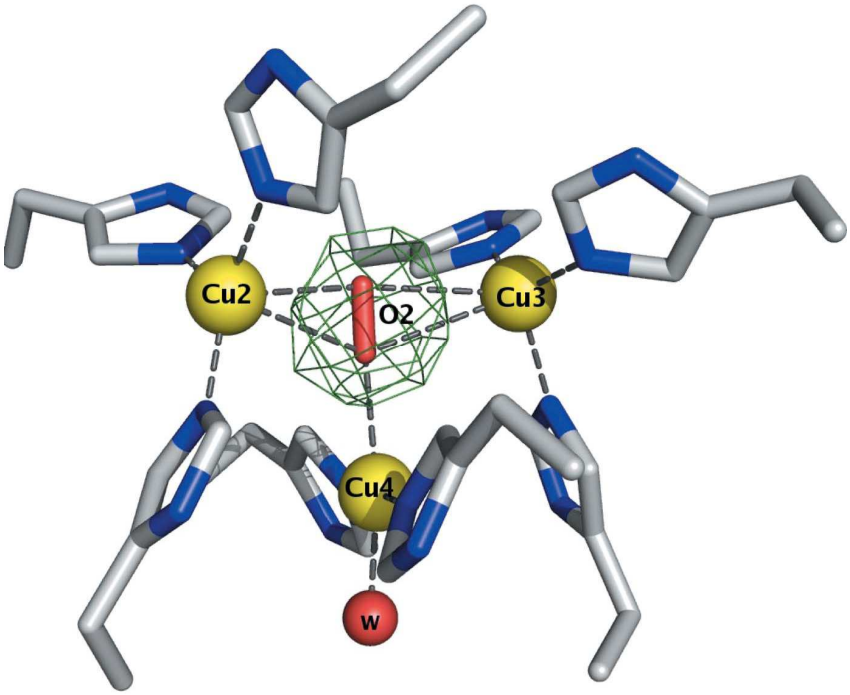

Figure 7. The trinuclear cluster between domains 1 and 6, showing the water molecule attached to the type 2 copper Cu4. An OMIT electron-density map, F_0-F_c, contoured at 7 r.m.s. clearly confirms the presence of a diatomic species, assumed to be dioxygen, within the type 3 cluster.

The separation of the two type 3 copper ions, Cu2—Cu3 4.97 Å, readily accommodates this species and it has been modelled as a dioxygen molecule in a similar manner to that found in the *Bacillus subtilis* endospore coat protein (Bento et al., 2005). A network of solvent molecules is found in the entrance channel to the trinuclear site, but some of these are weakly defined and may not

have full occupancies. Glu1032 may be the acidic residue necessary for the initial protonation of the dioxygen molecule via the water network.

The type 2 copper ion, Cu4, appears to have two configurations at around the 50% level, the first with an oxygen moiety O35, presumably hydroxide, at a distance of around 2.05 Å and the second with a water molecule, W148, at a distance of 2.98 Å.

According to the reaction scheme proposed by Bento et al. (Bento et al., 2005), both the hydroxyl group and the water molecule probably arise from reduction of a dioxygen at the trinuclear cluster.

GENE STRUCTURE AND EXPRESSION

Human ceruloplasmin is encoded in 20 exons encompassing approximately 65 kbp of DNA localized to chromosome 3q23-q24 (Daimon et al., 1995, Hellman and Gitlin, 2002). A processed pseudogene for human ceruloplasmin encoding the carboxyl-terminal 563 amino acids has been identified and mapped by somatic cell hybridization to chromosome 8 (Koschinsky et al., 1987). Although this pseudogene is not expressed, the presence of this sequence in the human genome must be considered in the design of any molecular diagnostic testing for aceruloplasminemia. In hepatocytes, the human ceruloplasmin gene is expressed as two transcripts of 3.7 and 4.2 kb, which arise from use of alternative polyadenylation sites within the 3' untranslated region (Koschinsky et al., 1986, Yang et al., 1986). Abundant expression of these transcripts in the liver results in the 1046–amino acid protein detected in serum. Nucleotide and amino acid sequence comparisons suggest that serum ceruloplasmin and the serum clotting factors V and VIII constitute a family of structurally related proteins (Church et al., 1984). Ceruloplasmin is an acute phase reactant, and the serum concentration increases during inflammation, infection, and trauma largely as the result of increased gene transcription in hepatocytes mediated by inflammatory cytokines (Gitlin, 1988).

Although the liver is the predominant source of serum ceruloplasmin, extrahepatic ceruloplasmin gene expression has been demonstrated in many tissues including spleen, lung, testis, and brain (Aldred et al., 1997, Fleming and Gitlin, 1990, Klomp et al., 1996, Yang et al., 1996). Within the human central nervous system ceruloplasmin is expressed in astrocytic glia lining the brain microvasculature, surrounding dopaminergic neurons in the substantia nigra, and within the inner nuclear layer of the retina (Klomp et al., 1996). Interestingly,

recent studies demonstrate that ceruloplasmin is synthesized as a glycophosphatidylinositol (GPI)-anchored protein generated by alternative splicing of exons 19 and 20 (Patel and David, 2000). This isoform has been identified prevalently in the brain, where it resides on the plasma membrane of astrocytes (Patel and David, 1997) and leptomeningeal cells (Mittal et al., 2003). Expression of ceruloplasmin-GPI has also been demonstrated in Sertoli cells (Fortna et al., 1999) and in the retina (Chen et al., 2003). Biosynthesis in these cell types suggests a role for this membrane-anchored form of ceruloplasmin in the oxidation and mobilization of iron at the blood-brain and blood-testis barriers. In addition to this GPI-linked isoform, a ceruloplasmin mRNA arising from alternative splicing of exon 18 and predicted to result in a protein with four additional amino acids has been detected in multiple extrahepatic cell types, although a protein product arising from this mRNA has not yet been characterized (Yang et al., 1990).

FUNCTION

In vitro ceruloplasmin is capable of catalyzing the oxidation of a number of different substrates, a finding that has created some confusion as to the physiologic role of this protein. Frieden demonstrated that ceruloplasmin from human serum had considerable ferroxidase activity and that this protein was able to mobilize iron from perfused dog livers with the subsequent oxidation of ferrous iron and incorporation of the ferric product into apotransferrin (Osaki et al., 1966, Osaki et al., 1971). In a series of elegant nutritional studies in pigs, Cartwright and his colleagues demonstrated that copper deficiency results in a marked decrease in circulating ceruloplasmin with concomitant iron accumulation in the liver and other tissues. The administration of oxidase-active ceruloplasmin to these animals resulted in the prompt release of iron into the circulation, which was detectable in circulating transferrin (Lee et al., 1968).

Although these biochemical and nutritional studies suggested a role for ceruloplasmin in iron homeostasis, the results were complicated by the presence of copper deficiency, which results in pleiotropic features.

Further evidence supporting a role for ceruloplasmin in iron homeostasis came from genetic studies designed to determine the mechanisms of iron uptake in yeast. High-affinity iron uptake in this organism is dependent upon the presence of the plasma membrane multicopper oxidase Fet3 (Askwith et al., 1994). This protein functions as a membrane ferroxidase, oxidizing iron in the

extracellular milieu for subsequent uptake by the membrane iron permease Ftr1 (Stearman et al., 1996).

Sla mice are affected with anemia secondary to impaired iron export from the intestine and placenta. Recognition that the defective gene in these animals encodes a multicopper oxidase with high homology to ceruloplasmin supported a role for these proteins in iron homeostasis in mammals (Vulpe et al., 1999). Definitive evidence in support of a physiologic role for ceruloplasmin in iron homeostasis came with the discovery of patients with aceruloplasminemia (Harris et al., 1995; Yoshida et al., 1995).

COPPER LOADING OF CERULOPLASMIN BY ATP7B

The liver is the central organ of copper homeostasis, and within the liver hepatocytes are the primary site of copper metabolism (Figure 8). Hepatocytes are highly polarized epithelial cells that regulate copper excretion into the bile dependent upon the intracellular copper concentration.

Human cells express two homologous Cu-ATPases: ATP7A and ATP7B (Lutsenko et al., 2007). These transporters use the energy of ATP hydrolysis to transport copper (in the reduced Cu^{+} form) from the cytosol across cellular membranes, thus decreasing cytosolic copper concentration. The transported copper is either released into the bloodstream for further distribution to tissues (in the case of ATP7A) or it is exported into the bile for eventual removal from the body (ATP7B). In addition to their copper export function, human Cu-ATPases are required for the delivery of copper cofactors to various copper-containing proteins. Secreted cuproproteins and the copper-containing proteins at the plasma membrane are thought to acquire their metal within the secretory pathway from the Cu-ATPases.

The loss of ATP7A or ATP7B function is associated with severe metabolic disorders, Menkes disease and Wilson disease.

Wilson disease is an autosomal recessive disorder resulting in hepatic copper accumulation. Identification of the molecular defect in this disorder has permitted a detailed understanding of the cell biological mechanisms of copper homeostasis (Loudianos and Gitlin, 2000). Wilson disease results from the absence or dysfunction of ATP7B. This ATPase transports copper into the secretory pathway for subsequent incorporation into ceruloplasmin and excretion into bile. When the copper concentration in the hepatocyte increases, the Wilson

ATPase traffics from the *trans*-Golgi network to a cytoplasmic vesicular compartment near the canalicular membrane. Copper is then sequestered in this vesicular compartment, and as the cytoplasmic copper concentration decreases, the Wilson ATPase returns to the *trans*-Golgi network while copper is excreted at the biliary canaliculus (Hung et al., 1997).

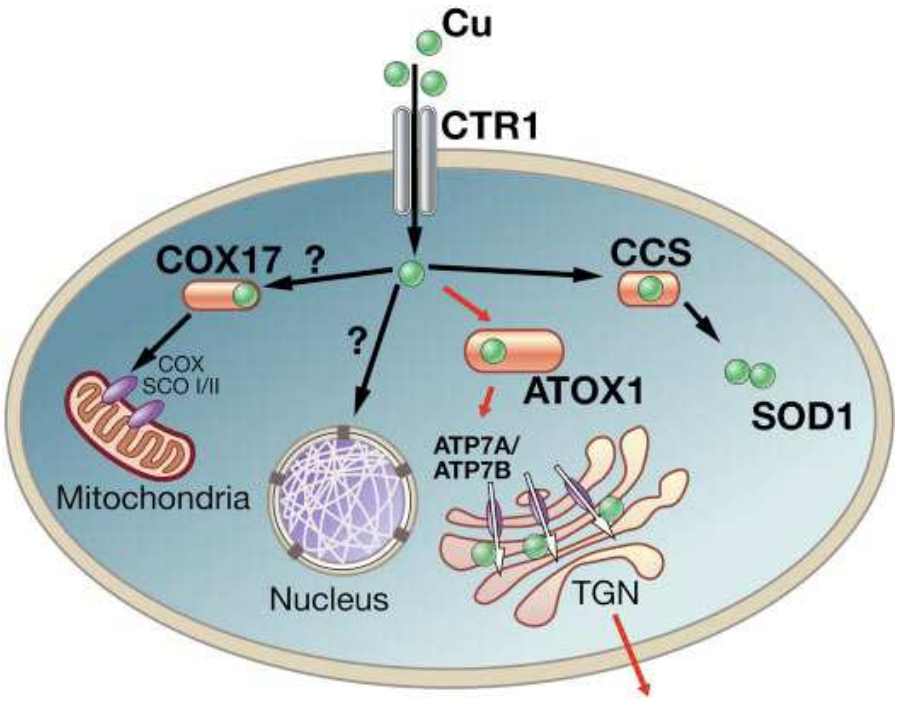

Figure 8. Intracellular pathways of copper distribution. Copper enters the cell through the high-affinity copper transporter Ctr1 and binds to cytosolic copper chaperones. Cox17 may participate in delivery of copper to the mitochondrion, although this role has recently been questioned, and together with Sco proteins facilitates incorporation of copper into cytochrome-*c* oxidase (COX). CCS transfers copper to cytosolic SOD1. The red arrows indicate the pathway in which Cu-ATPases play the major role. In this pathway, Cu-ATPases receive copper from ATOX1, transfer copper into the lumen of the secretory pathway, and also export excess copper from the cell.

This copper-dependent movement of the Wilson ATPase provides for a unique post-translational mechanism that permits rapid and sensitive regulation of copper homeostasis by hepatocytes. This mechanism also accounts for the

observation that loss-of-function mutations in the Wilson gene result in impaired biliary copper excretion and decreased serum ceruloplasmin.

Genetic and biochemical studies of *Saccharomyces cerevisiae* indicate that under physiological conditions intracellular copper availability is extraordinarily restricted (Rae et al., 1999). For this reason the delivery of copper to specific targets within the cell is mediated by a family of proteins termed copper chaperones that provide copper directly to specific proteins while protecting it from intracellular scavenging (Rosenzweig, 2000).

The cytoplasmic copper chaperone atox1 is required for the delivery of copper to the secretory pathway via direct interaction with the Wilson ATPase in the *trans*-Golgi network (Larin et al., 1999). Atox1 is thus directly in the pathway of copper delivery to ceruloplasmin; consistent with this, mice deficient in atox1 demonstrate increased mortality with evidence of impaired copper incorporation into cuproproteins in the secretory pathway of most cells (Hamza et al., 2001).

The mechanism of copper incorporation into ceruloplasmin is not well defined. Fractionation studies and pulse-chase experiments indicate that copper is incorporated into ceruloplasmin late in the secretory pathway either at or beyond the *trans*-Golgi network (Terada et al., 1995). Recent studies of a missense mutation that results in retention of ceruloplasmin in the endoplasmic reticulum support this concept and indicate that copper is not incorporated into nascent apoceruloplasmin in this compartment (Hellman et al., 2002). Because quality control mechanisms ensure proper folding of newly synthesized ceruloplasmin prior to exiting the endoplasmic reticulum, these data on the site of copper incorporation suggest that additional events must occur to allow for metal acquisition by apoceruloplasmin late in the secretory pathway. Genetic studies of *S. cerevisiae* demonstrate a requirement for both the ATP7B-homologue Ccc2p and the CLC chloride channel Gef1 for copper incorporation into the homologous multicopper oxidase Fet3 (Gaxiola et al., 1998). Analogously, copper loading of ceruloplasmin appears to be chloride-dependent and over-expression of the chloride channel CLC-4 in *trans*-Golgi vesicles was found to be related to an increase of secreted holo-Cp (Wang and Weinman, 2004). Further work is needed to elucidate this process and to determine if common mechanisms exist for all cuproproteins in the secretory pathway.

ACERULOPLASMINEMIA: AN IRON OVERLOAD DISEASE

Aceruloplasminemia is an autosomal recessive neurodegenerative disease characterized by iron accumulation in the brain as well as visceral organs. It is a loss-of-function disorder caused by mutations in the ceruloplasmin gene. Clinically, this disease consists of the triad of adult-onset neurological disease, retinal degeneration and diabetes mellitus. Laboratory findings include absence of serum ceruloplasmin ferroxidase activity (although low levels of ceruloplasmin protein were reported in some cases), low transferrin saturation, high serum ferritin and moderate anemia; magnetic resonance imaging of the brain shows iron deposits in the basal ganglia, striatum, thalamus and dentate nucleus.

Individuals heterozygous for the disease mutations have a partial Cp deficiency and usually display normal iron metabolism and no clinical symptoms, although a few cases of affected heterozygous patients have been reported. Homozygotes, however, show symptoms of iron overload disease; about 40 published mutations (including frameshift, nonsense, and missense mutations) in 45 pedigrees have been described, as reported on-line (Figure 9).

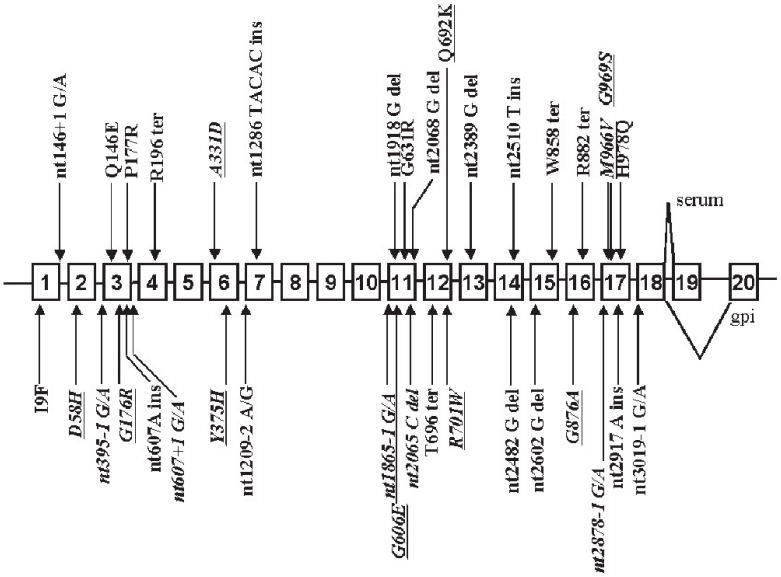

Figure 9. Aceruloplasminemia-causing mutations in the ceruloplasmin gene (from Kono and Miyajima, 2006).

Aceruloplasminemia does not result in impaired intestinal iron uptake and transport, as the oxidation of iron necessary for this process is accomplished by the homologous multicopper oxidase hephaestin (Vulpe et al., 1999). The impairment of iron homeostasis in patients with aceruloplasminemia is best understood by examining the role of ceruloplasmin in the systemic iron cycle (Andrews, 1999) (Figure 10).

Most of the iron used each day for hematopoiesis and other essential needs is recycled from heme as erythrocytes are turned over within the reticuloendothelial system. Iron transported in the plasma bound to transferrin must be oxidized prior to binding to this transport protein. Ceruloplasmin plays a critical role in the iron cycle by establishing a rate of iron oxidation sufficient for iron release from the reticuloendothelial system.

The absence of serum ceruloplasmin in patients with aceruloplasminemia leads to a slow accumulation of iron in compartments where this metal is normally mobilized for recycling. This concept can be readily appreciated in a murine model of aceruloplasminemia in which an experimental situation is created in which either excess iron is delivered to the reticuloendothelial system or the hematopoietic requirement for iron is increased by phlebotomy (Harris et al., 1999).

Consistent with these observations, the administration of ceruloplasmin as fresh frozen plasma to patients with aceruloplasminemia results in a rapid increase in serum iron (Logan et al., 1994). Analysis of these experimental findings also illustrates why phlebotomy is an inappropriate and harmful approach to the iron overload in aceruloplasminemia.

Patients with aceruloplasminemia have only mild anemia and are able to maintain the iron cycle to a degree sufficient for hematopoiesis, presumably owing to alternative oxidase sources in the plasma.

In addition to the slow accumulation of iron within the reticuloendothelial system, the absence of serum ceruloplasmin also results in increased ferrous iron in the plasma, which is rapidly removed from the circulation by the liver, pancreas, and other tissues. This process is analogous to what occurs in patients with atransferrinemia, in which serum transferrin is absent, or primary hemochromatosis, in which transferrin binding capacity is exceeded (Craven et al., 1987). This non-transferrin dependent iron uptake is presumably mediated by DMT1, the divalent cation transporter expressed in most tissues, which has been shown to be required for normal intestinal iron uptake (Andrews, 2000). This mechanism of iron uptake accounts for the

accumulation of iron in hepatocytes and pancreatic β-cells observed in patients with aceruloplasminemia. In most situations 5% of the circulating serum ceruloplasmin is sufficient to sustain a normal plasma iron turnover rate, which is why abnormalities of iron homeostasis are rarely observed in patients with Wilson disease (Roeser et al., 1970). Although ceruloplasmin is required for the efficient release of cellular iron, the actual mechanism of transport of iron from cells is mediated by the polytopic membrane protein ferroportin (Figure 10).

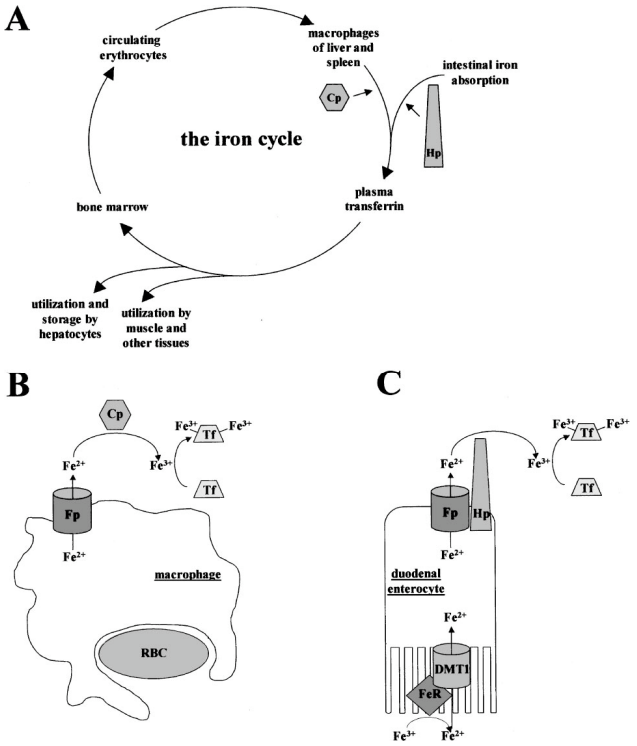

Figure 10. Role of the multicopper oxidases in the iron cycle. (*A*) The iron cycle is depicted with movement of iron between sites of storage and utilization. (*B*) In the reticuloendothelial system (macrophage) iron derived from heme is returned to the plasma via the membrane transporter ferroportin (Fp). Ceruloplasmin (Cp) plays an essential role in determining the rate of iron efflux via oxidation, which is required for binding to transferrin (Tf). (*C*) Iron absorption in the enterocyte requires the apical membrane reductase (FeR) and the divalent metal transporter-1 (DMT1), as well as the basolateral transporter Fp and the ceruloplasmin homologue hephaestin (Hp). The role of hephaestin in enterocyte iron efflux is analogous to that of ceruloplasmin in the reticuloendothelial system.

ACERULOPLASMINEMIA IN THE CENTRAL NERVOUS SYSTEM

The elevated iron concentration is associated with increased lipid peroxidation in the brains of aceruloplasminemia patients. Massive iron accumulation and extensive loss of neurons are observed in the basal ganglia. Enlarged or deformed astrocytes and spheroid-like globular structures are characteristic neuropathological findings in aceruloplasminemia. Moreover, deformed astrocytes and globular structures react positively to anti-4-hydroxynonenal antibody, suggesting that increased oxidative stress is involved in neuronal cell death in aceruloplasminemia brain (Kono et al., 2006).

Characteristic pathological features of aceruloplasminemia are progressive neurodegeneration of basal ganglia in association with iron accumulation in these tissues. Ceruloplasmin may play an important role in normal brain iron homeostasis. Under normal circumstances, circulating Cp does not cross the blood-brain barrier. Iron is taken into the brain tissues from the circulation through receptor-mediated endocytosis of transferrin. Iron may be oxidized by GPI-linked Cp expressed in the astrocytes, incorporated into transferrin derived from the oligodendrocytes, and transferred to the neuronal cells. In the absence of Cp, iron is accumulated in the brain cells.

As described in the section on ferroportin, recent data have demonstrated that the ferroxidase activity of ceruloplasmin is required for the stability of cell surface ferroportin, the only known mammalian iron exporter, and that ferroportin is rapidly internalized and degraded in the absence of ceruloplasmin (De Domenico et al., 2007). This finding provides a straightforward explanation for brain iron overload in patients with aceruloplasminemia, where the lack of a functional ceruloplasmin-GPI would lead to defective export of iron from cells because of degradation of ferroportin.

NEURODEGENERATION AND GOLGI FRAGMENTATION

The Golgi apparatus is a cytoplasmic organelle involved in the transport, processing, and targeting of proteins synthesized in the rough endoplasmic reticulum and destined for the secretory pathway. In normal cells, the Golgi apparatus is composed of a series of flattened, parallel, interconnected cisternae organized around the microtubule-organizing center in the perinuclear region. The Golgi apparatus was originally thought to be a static organelle, but it is

actually a highly dynamic structure. Examples of the Golgi's dynamic behavior include its reversible disassembly during mitosis, when the Golgi apparatus fragments to produce clusters of vesicles that disperse throughout the cytoplasm (Robbins and Gonatas, 1964; Warren, 1993). These mitotic Golgi fragments are equally partitioned into the daughter cells. Upon exit from the mitotic program, the perinuclear Golgi apparatus is reconstituted simultaneously with the reformation of the nuclear envelope.

Recent reports show that inhibition of Golgi fragmentation prevents entry into mitosis, suggesting that Golgi fragmentation is not merely a response to mitosis but a causal event in the process (Sutterlin et al., 2002).

Since the Golgi apparatus is involved in numerous important functions, such as the transport, processing, and targeting of proteins synthesized in the endoplasmic reticulum (ER), quality control of proteins in the Golgi apparatus and ER must be stringent to ensure appropriate cellular function. Thus, fragmentation of Golgi during cell death might have detrimental effects and lead to dysfunction of the cytoplasmic machinery in neurons as well as in non-neuronal cells. Along these lines, fragmentation of the Golgi apparatus has been reported in vivo in several human neurodegenerative diseases, including Alzheimer's disease (AD) and amyotrophic lateral sclerosis (ALS) (Gonatas et al., 2006).

Nakagomi et al. (2008) found that several types of neuronal insult induce Golgi fragmentation, including excitotoxicity, reactive oxygen or nitrogen species, and ER stress. Importantly, pharmacological or molecular inhibition of Golgi fragmentation and dispersal decreased or delayed apoptotic-like cell death, implicating a causal effect of the Golgi apparatus in these cell death pathways. The authors also found that molecular interference with mitochondrial- or ER-mediated apoptotic pathways partially abrogates Golgi fragmentation and neuronal cell death, suggesting that these other organelles are upstream in the cell death pathway in response to their apoptotic effectors.

AIM OF THE WORK

The multicopper oxidase ceruloplasmin plays a key role in iron homeostasis, and its ferroxidase activity is required to stabilize cell surface ferroportin, the only known mammalian iron exporter.

In this work, missense mutations causing the rare autosomal neurodegenerative disease aceruloplasminemia have been investigated by testing their ability to prevent ferroportin degradation in rat glioma C6 cells silenced for endogenous ceruloplasmin. Functional characterization of mutant ceruloplasmins has been performed in parallel by using the yeast *Pichia pastoris* as a host for heterologous ceruloplasmin production.

Our study is focused on physiological mutant ceruloplasmin R701W, which was found in a heterozygous very young patient with severe neurological problems. Arg-701 is located in a large solvent-exposed loop connecting domains 4 and 5 of ceruloplasmin, and corresponding loops connect the other domains of the protein. Despite a low degree of sequence homology, all these loops start with a C-X-R/K motif, with the cysteine residue stabilizing the loop by forming a disulphide bridge.

We have investigated the role of these external loops of human ceruloplasmin in copper loading by the Cu ATPases ATP7B and Ccc2p in C6 rat glioma cells and in yeast.

Further we have investigated, in our cell culture model system, the possible molecular mechanisms underlying the severe neurological problems that characterize this form of aceruloplasminemia.

MATERIALS AND METHODS

Constructs

The cDNA for human Cp-GPI was cloned by RT-PCR on total RNA from U373MG human glioma cells with the cMaster RT-PCR System (Eppendorf). The secreted form of Cp was generated by PCR by substituting the region coding for the last 30 residues of the GPI-anchored isoform with the five amino acids of secreted Cp. For expression in mammalian cells, the Cp-GPI or secreted Cp cDNA was cloned SacI-XhoI in the pCMVTag4b vector (Stratagene). For expression in yeast the secreted Cp cDNA was cloned SacI-XhoI in the pIB2 vector (Sears et al., 1998), under control of the constitutive GAP promoter. All mutants were produced either with the QuikChange II XL mutagenesis kit (Stratagene) or by megaprimer PCR. The FLAG or Myc tag was introduced by PCR in the coding sequence of Cp to replace Arg-481. *Saccharomyces cerevisiae* and *Pichia pastoris* Ccc2p coding sequence were obtained by PCR on genomic DNA and cloned EcoRI-XhoI or BamHI-XhoI in pCMVTag4b to generate a C-terminally FLAG-tagged protein. All constructs were verified by automated DNA sequencing at Biogen-ENEA (Italy). The pFpn-EGFP expression plasmid was a generous gift from J. Kaplan.

Cells and Media

Rat C6 glioma cells were purchased from the ATCC and maintained in Dulbecco's modified Eagle's medium (Sigma) supplemented with 10% fetal bovine serum (Cambrex) and 40 μg/ml gentamicin (Sigma). Confluent monolayers were subcultured by conventional trypsinization, and cells were seeded in 35-mm tissue culture dishes for transfections.

Small Interfering RNA (siRNA) and Transient Transfection

siRNA oligonucleotide pool matching selected regions of rat Cp-GPI was obtained from Dharmacon (ON-TARGETplus SMART pool L-089853) and was specific for the rat protein, allowing expression of transfected human Cp isoforms (both GPI and secreted).

Sense sequences of oligonucleotide pools were as follows:

gaaaugguccagaucguauuu;
gaaugaaguugacgugcauuu;
gaaugaaucuugguacuuauu;

ggagaaaggaccuacuauauu.
siRNA oligonucleotide pool matching selected regions of rat ATP7B was obtained from Qiagen.
Sense sequences of oligonucleotide pools were as follows:
ggugacaucgaacugauuatt
guuagaaagcacuaaccuatt
C6 cells were transfected with siRNAs at a final concentration of 100 nM by using Oligofectamine (Invitrogen). Eighteen to 24 h after silencing, cells were transfected with pFpn-EGFP and pCMVhCp constructs using Lipofectamine enhanced by the Plus reagent (Invitrogen). Cells were grown for 18–24 h and then processed for immunofluorescence microscopy or Western blot analysis.

Immunofluorescence Microscopy
Cell staining for immunofluorescence microscopy was performed as described previously (De Domenico et al., 2007), using the following primary antibodies: rabbit anti-Cp (1:100, Dako), mouse anti-FLAG M2 (1:100, Sigma), mouse anti-Myc 9E10 (1:100, Santa Cruz Biotechnology), mouse anti- TGN-38 (1:50, BD Biosciences), mouse anti-GM130 (1:50, BD Biosciences), mouse anti-Mannosidase II (1:10000 Covance), rabbit anti-ATP7A/B (1:50, Santa Cruz Biotechnology or Novus Biologicals), rabbit anti-FLAG (1:100, Sigma), rabbit anti-Giantin 1:1000 (Novus Biologicals), and rabbit anti-Myc (1:100, Sigma), followed by treatment with either Alexafluor 594- or fluorescein isothiocyanate-conjugated goat anti-rabbit IgG (1:750, Invitrogen), or Alexafluor 594-conjugated goat anti-mouse IgG (1:750, Invitrogen) as secondary antibodies.
NBD-C6-ceramide complexed to bovine serum albumin (Invitrogen Molecular Probes) was used, following the manufacturer's instructions, to produce selective staining of the Golgi complex for visualization by fluorescence microscopy.
Lysotracker DND-99 (Invitrogen Molecular Probes) has been used according to the manufacter's instructions.
Cells were visualized using an inverted DMI 6000 confocal scanner microscope TCS SP5 (Leica Microsystems CMS GmbH) with a 63X oil immersion objective. Images were acquired using Leica application suite advanced fluorescence software. Each fluorochrome was scanned individually, and each image included 3–8 cells. The number of cells showing a certain pattern was counted in every image and expressed as a percentage of all cells in the image. Then the median percentage from different images was calculated.

Western Blot

The Cu(I)-glutathione complex was prepared as described previously (Musci et al., 1996). For Western blot analysis of secreted Cp, culture supernatants of transfected cells grown in serum-free medium were supplemented with protease inhibitors (PMSF 1 mM, leupeptin 2 μg/ml, pepstatin 2 μg/ml), concentrated with Microcon 30 devices (Millipore), and fractionated by SDS-PAGE under denaturing (samples heated in the presence of reducing agents) or nondenaturing (samples loaded as such) conditions. This technique was used to discriminate apo- and holo-Cp, as reported (Sato and Gitlin, 1991). For analysis of Cp-GPI, cells were solubilized in 25 mM MOPS buffer (pH 7.4), 150 mM NaCl, 1% Triton X-100, supplemented with protease inhibitors, by incubation on ice for 45 min. Protein content of cell extracts was determined by either the microBCA method (Pierce) or Bradford assay (Bio-Rad). Equal amounts of lysates were fractionated by SDS-PAGE, transferred to nitrocellulose, and probed with rabbit anti-Cp antibody (1:5000, Dako), mouse anti-FLAG M2 (1:2000, Sigma), mouse anti-Myc 9E10 (1:1000, Santa Cruz Biotechnology), and rabbit anti-ATP7A/B (1:500, Santa Cruz Biotechnology) antibodies. The appropriate peroxidase-conjugated secondary antibody (Sigma) was used at a 1:10000 dilution. The blot was visualized with ECL Plus (GE Healthcare) or Blue POD (Roche Applied Science).

Measurement of Reactive Oxygen Species

2',7'-dichlorodihydro-fluorescein diacetate (H_2DCF-DA; Invitrogen), a redox-sensitive probe was used to determine intracellular ROS levels (Bacsi et al., 2005; Boldogh et al., 2003). H_2DCF-DA is converted to the membrane-impermeant polar derivative H_2DCF by esterases when it is taken up by the cell. H_2DCF is non fluorescent but is rapidly oxidized to the highly fluorescent DCF by intracellular H_2O_2 and other peroxides (Genty et al., 1989). For assessment of ROS, the samples were loaded with 1 mL of 5 μM DCFH-DA (dissolved in DMSO) in PBS buffer and maintained at 37°C in the dark for 60 min. At the end of the incubation period, loading buffer was removed and C6 cells were incubated at 37°C for additional 30 min in prewarmed growth medium. For derivatives with acetoxymethyl ester (AM) and/or diacetate groups, a short recovery time for cellular esterases to hydrolyze the AM or acetate groups and render the dye responsive to oxidation is in fact necessary.

N-Acetyl-Cysteine (NAC) and reduced glutathione (GSH) were dissolved in water at a stock concentration 0.5 M. Final concentration used on cell cultures

was 2 mM and the reagents were added in the transfection mix.

Expression, purification and characterization of recombinant Cp in Yeast

The expression plasmids with the Cp cDNA were linearized with *Sal*I and electroporated in the *P. pastoris fet3*Δ strain (*ade1, his4, arg4, fet3::ADE1*). The presence of Cp was confirmed by PCR on genomic DNA of selected His^+ colonies. Expression of secreted Cp was performed in MD buffered with 50 mM potassium phosphate pH 6 supplemented with arginine 5 μg/ml, $CuSO_4$ 100 μM and $Fe(NH_4)_2(SO_4)_2$ 50 μM. Yeast cells were grown overnight at 25-28°C to OD_{600} 2.5-3.5, 0.1 mM PMSF was added to the suspension and the culture supernatant was recovered by pelleting cells at 3500 *g* for 10 min. The culture supernatant was filtered, diluted 1:2.5 with deionized water and brought to pH 7.4. Cp was partially purified by chromatography on DEAE-Sephacell (GE Healthcare) equilibrated in 25 mM MOPS pH 7.4, containing 50 mM NaCl. About 7.5 ml resin were used per liter of undiluted culture medium. The resin was sequentially washed with 3 volumes of MOPS buffer, containing 50-100-120-150 and 500 mM NaCl. Cp was eluted at 150 mM NaCl and Cp-containing fractions were concentrated with Amicon Ultra 15 devices with molecular weight cut-off 30 kDa.

Denaturing and non-denaturing SDS-PAGE, staining for oxidase activity with o-dianisidine and Western blot were performed as described above.

Oxidase activity was assayed with o-dianisidine according to Schosinsky et al. (1974). Briefly, activity was determined in the presence of 1.58 mM o-dianisidine in 0.5 ml of 100 mM sodium acetate buffer pH 6 at 37°C for 60 min; the reaction was stopped by addition of 0.5 ml H_2SO_4 9 M and the amount of product was determined by absorbance at 540 nm.

Deglycosylation with endoH (New England Biolabs) was performed in denaturing conditions, according to the manufacturer's instructions.

Indirect ELISA was performed for quantification of recombinant Cp. Dilutions of purified human Cp 0.6 mg/ml as standard curve were used to interpolate samples Cp concentrations. All steps used a volume of 100 μl/well and were carried out at room temperature, unless otherwise indicated. Polystyrene 96-well microplates were coated overnight at 4°C with either standard Cp in duplicate (1:4,000; 1:8,000; 1:16.000; 1:32,000; 1:64,000), samples (1:1,000; 1:2,000; 1:4,000), or blank in Phosphate-buffered saline, pH 7.2. Solution was then removed and the wells were washed three times with Phosphate-buffered saline containing Tween 20 0.05%. This buffer was used for all subsequent washing

steps and antibody dilutions. A 30-min incubation at 37°C with 1% bovine serum albumin ensured complete saturation of unoccupied centers of sorption. Three washings were performed and 1 μg/well of goat polyclonal anti-Cp (Sigma) as primary antibody was added. After 1-h antibody solutions were washed and 1:3000 anti-Goat IgG horseradish peroxidase conjugated (Sigma) was used as secondary antibody. After 1-h of incubation three more washings were carried out and ABTS, containing 1 mM H_2O_2 was added. After 10 min A_{405} was measured in a microplate reader (Wallac Victor, Perkin Elmer). Data analysis and curve fitting were performed with GraphPad Prism software.

RESULTS

MISSENSE ACERULOPLASMINEMIA MUTANTS CAN OR CANNOT COMPLEMENT SILENCING OF ENDOGENOUS CERULOPLASMIN

Among the aceruloplasminemia missense mutants described up to now, only a few have been characterized (Hellman et al., 2002; Kono et al., 2006). Fundamental contributions to the understanding of the molecular basis of this pathology revealed that the mutants were retained totally (P177R) or partially (I9F) in the early secretory pathway of cells, or they were secreted as an inactive apo-protein lacking copper (G631R and G969S). It can be inferred from the X-ray structure of Cp that also other substitutions are expected to perturb copper incorporation because the mutated residues are either copper ligands (His-978) or they are close to copper-binding sites (Ala-331 and Gln-692).

The effect of the other mutations on the structure and activity of Cp appears to be less predictable. In particular, mutation R701W is very intriguing because it has been found in an atypical very young heterozygous patient with extremely severe neurologic symptoms despite the presence of the wild type allele (Kuhn et al., 2005). Arg-701 is located in a long surface exposed loop on the flat basal region of Cp, making it difficult to correlate the disease phenotype to a folding or ferroxidase activity defect of the protein.

Ferroxidase-competent Cp is required to maintain Fpn on the plasma membrane (De Domenico et al., 2007). Therefore, the ability of missense aceruloplasminemia mutants to prevent Fpn degradation represents a valid test of the functionality of the mutated protein. Because brain iron overload is a hallmark of aceruloplasminemia, we chose the rat C6 glioma cell line as our model system. Oligonucleotides selective for rat Cp were used to silence C6 cells for endogenous Cp-GPI, and cells were co-transfected with mouse Fpn-GFP and with human WT or mutant Cp-GPI (hCp-GPI). Then the presence of Fpn-GFP was assessed by epifluorescence microscopy 48 h after silencing.

As already reported (De Domenico et al., 2007), hCp WT was able to restore Fpn on the membrane (Fig. 1A). On the other hand, the Cp missense mutants were found to fall into three categories as follows: fully functionally competent, partially competent, or functionally incompetent. Epi- and immunofluorescence fields obtained on selected mutants representative of the three categories are shown in Fig. 1A.

Mutants known to be enzymatically inactive (P177R, G631R, and G969S) and mutants D58H, Q692K, and R701W were unable to rescue Fpn-GFP; mutations F198S and A331D restored Fpn-GFP on 40–60% of cells, whereas mutations I9F, Q146E, W264S, G606E, and G876A fully complemented the silencing of endogenous Cp-GPI. Identical results were obtained by transfecting the corresponding soluble isoforms of hCp (data not shown).

All hCp-GPI mutants except P177R, which was found in the ER, as expected (Hellman et al., 2002), correctly localized to the plasma membrane, and Western blot analyses demonstrated that endogenous Cp-GPI was fully silenced under our conditions (Fig. 1B), its synthesis being mostly inhibited even 72 h after addition of the silencing oligonucleotides.

All recombinant hCp-GPI proteins were expressed at comparable levels (Fig. 1C). The apo/holo status of transfected hCp mutants was evaluated by non-denaturing SDS-PAGE, i.e. without heat treatment and in the absence of reducing agents prior to loading samples on the gel. Fig. 1D reports the results on the mutants depicted in Fig. 1A. The soluble isoform of the protein had to be employed in this experiment, because of instability of the GPI-linked isoform in these conditions.

The results indicated that the ability of the mutants to rescue (totally or in part) Fpn-GFP was related to the presence of holo-hCp, which runs as a band at 85 kDa versus apo-hCp at 130 kDa (Sato and Gitlin, 1991), as exemplified by the lanes of I9F and F198S in Fig. 1D. On the other hand, only the apo-protein form was detected for functionally incompetent mutants Q692K, R701W (Fig. 1D), D58H, and G631R.

The amount of secreted hCp turned out to be much higher in samples where most of the protein was holo. Because it is known that the rate of synthesis and secretion of wild type Cp is the same for the holo- and the apo-forms (Hellman et al., 2002), these data suggest that secreted apo-hCp is unstable; however, the hypothesis that soluble mutants synthesized as apo-protein are poorly secreted compared with wild type cannot be ruled out.

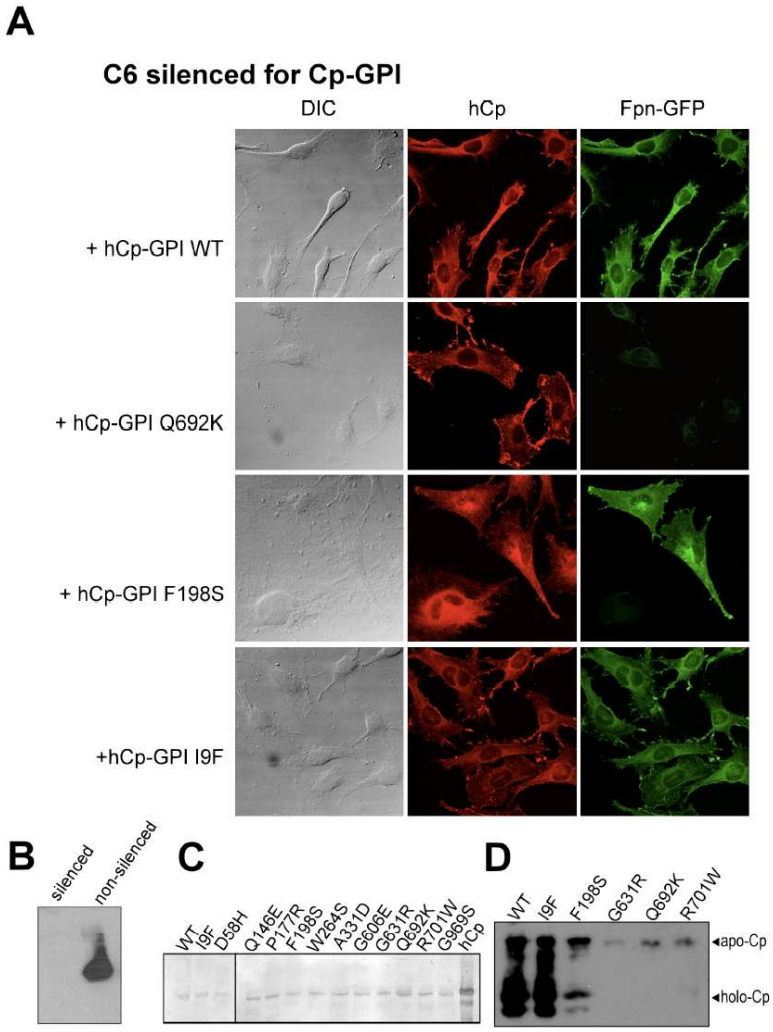

Figure 1. **Functional complementation by hCp-GPI missense mutants.** *A*, rat glioma C6 cells were silenced for Cp-GPI. After 24 h they were transfected with Fpn-GFP and human Cp-GPI WT, Q692K, F198S, or I9F and analyzed after a further 24 h by epifluorescence (*Fpn-GFP*) and immunostaining (*Cp*). *DIC*, differential interference contrast. *B*, Western blot analysis for Cp on silenced or non-silenced cell extracts, and equal amounts of total protein (150 μg) were loaded per lane. Cells were silenced 48 h before preparing the cell extracts. *C*, cell extracts from C6 cells silenced for Cp-GPI and transfected with the indicated human Cp-GPI were examined for Cp by Western blot analysis, and equal amounts of total protein (30 μg) were loaded per lane. *D*, culture supernatants from C6 cells silenced for Cp-GPI and transfected with the indicated human secreted Cp were concentrated 10-fold and analyzed by non-denaturing SDS-PAGE and Western blot to evidence holo-hCp (85 kDa) and apo-hCp (130 kDa).

CP R701W IS DOMINANT OVER CP WT

The next step was to investigate whether mutants synthesized as apo-Cp lacked copper because of structural defects. To this purpose, in situ reconstitution of secreted hCp with the Cu(I)-GSH complex, which has been shown to remetallate apo-Cp in vitro (Musci et al., 1996), was attempted. Cells were silenced for endogenous Cp-GPI and transfected with the soluble form of hCp WT, D58H, Q692K, or R701W.

Consistent with previous data (De Domenico et al., 2007), transfected soluble hCp WT was able to rescue Fpn-GFP.

Cu(I)-GSH was ineffective on untransfected silenced cells and on cells transfected with hCp D58H or Q692K; the latter is shown in Fig. 2. On the other hand, addition of Cu(I)-GSH to the medium restored Fpn-GFP on about 30–40% of cells transfected with secreted hCp R701W (Fig. 2), suggesting that in this case the secreted protein lacks copper but retains the ability to bind it.

Consistently, Western blot analysis confirmed that, at variance with Q692K, apo-hCp R701W was partly converted to holo-hCp R701W by Cu(I)-GSH (Fig. 2).

The amount of secreted apo-Cp appeared to be higher in samples where Cu(I)-GSH was present, irrespective of the mutant used. This could be due to a general stabilizing effect of added copper or to a positive effect of the complex on Cp secretion. Human Cp D58H appeared to be partially reconstituted by Cu(I)-GSH, despite lack of Fpn-GFP recovery.

Therefore, hCp R701W is unique in that it does not possess a structural defect, which makes it intrinsically unable to bind copper, and that an active enzyme can be produced under proper conditions.

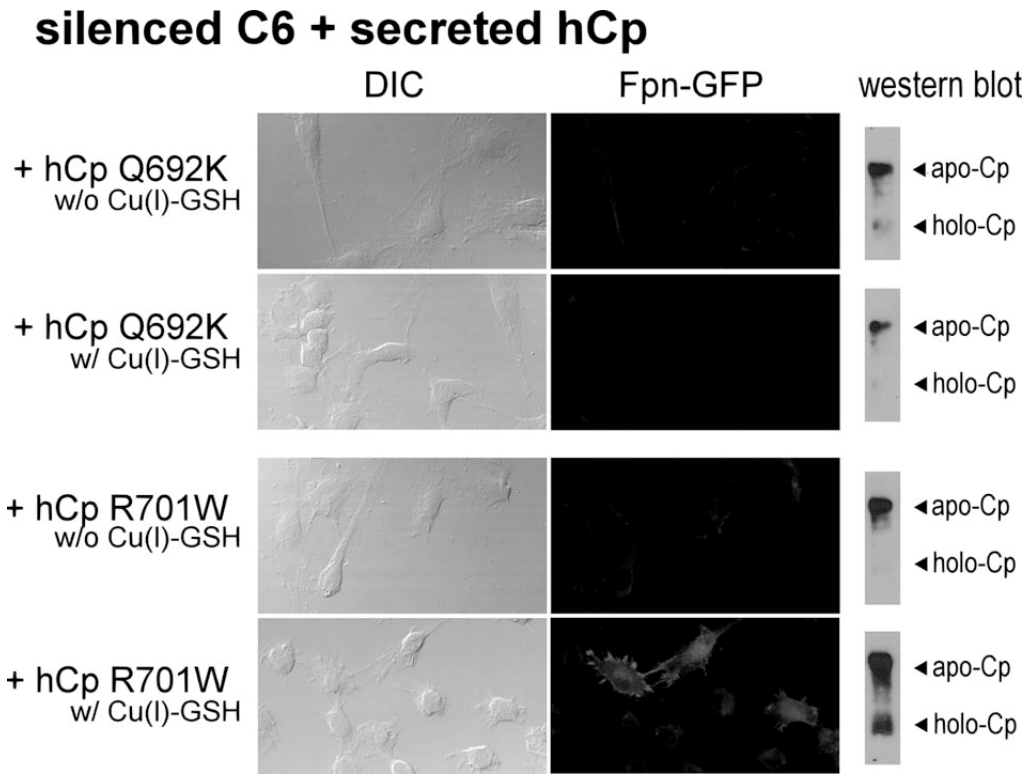

Figure 2. The copper-glutathione complex reconstitutes a functional hCp R701W. Cells were silenced for Cp-GPI, transfected with Fpn-GFP and secreted hCp R701W or Q692K, and then examined by epifluorescence after 24 h in the absence or presence of 50 μM Cu(I)-GSH complex in the medium. The corresponding Western blot analysis run after nondenaturing SDS-PAGE to distinguish apo- and holo-Cp is shown beside each fluorescence set. *DIC*, differential interference contrast.

Quite strikingly, hCp R701W was dominant over Cp WT. This was first assessed on non-silenced cells, as shown in Fig. 3A. Clearly, Fpn was degraded when cells were transfected with hCp-GPI R701W, despite the presence of endogenous Cp (Fig. 3A).

The same result was obtained when non-silenced cells were transfected with the soluble form of hCp R701W. The dominance of R701W mutation over the wild type protein was maintained when cells were silenced for endogenous Cp and transfected with hCp WT (both soluble and GPI linked). Again, no Fpn was observed in the presence of hCp R701W irrespective of the simultaneous

presence of the WT protein (Fig. 3B).

R701W was the only natural mutation found to have this property. As a matter of fact, rescue of Fpn-GFP by hCp WT was not affected by co-expression of any other functionally incompetent mutant, as exemplified by the Q692K mutant in Fig. 3B.

The mechanism of dominance of Cp R701W on WT was then investigated. To this purpose, the effect of Cu(I)-GSH was first studied. Silenced cells were co-transfected with hCp-GPI R701W and secreted hCp WT, and the protein recovered in the medium was analyzed by Western blot after non-denaturing SDS. As shown in Fig. 3C, upper panel, the secreted hCp WT was mostly in the apo-form, which could be partially converted to holo-form in the presence of Cu(I)-GSH (lower panel). The fluorescence analysis confirmed that a significant fraction of cells recovered Fpn-GFP in the presence of Cu(I)-GSH. Altogether, these data indicate that the presence of the mutant R701W impairs copper loading of co-transfected hCp WT and that copper loading is partially restored by Cu(I)-GSH, with consequent recovery of Fpn-GFP. Moreover, the efficiency of reconstitution of Cp by the Cu(I)-GSH complex is similar for both Cp WT and R701W (cf. the Western blots in Figs. 2 and Fig. 3C), leading to a similar extent of recovery of Fpn-GFP.

Consistently, the same effect of Cu(I)-GSH was observed when silenced cells were co-transfected with secreted hCp R701W and hCp-GPI WT.

These findings are particularly relevant because R701W is found in a heterozygous atypical very young patient. Thus, this mutant was further investigated, to better elucidate the origin of the failure of copper loading leading to the dominant negative phenotype.

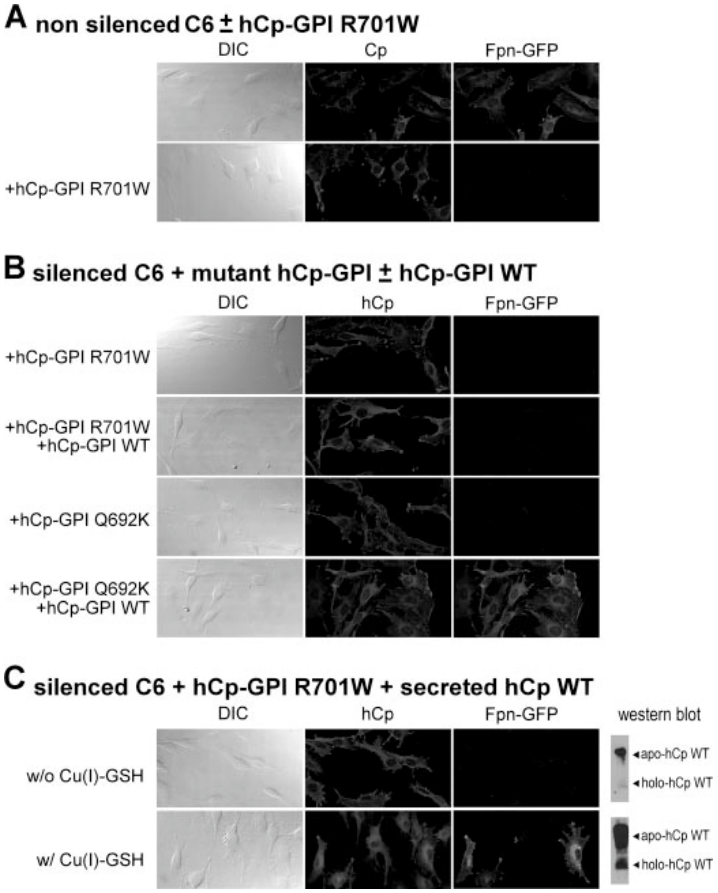

Figure 3. Human Cp R701W is dominant over Cp WT. *A,* C6 cells were co-transfected with Fpn-GFP and hCp-GPI R701W and then examined after 24 h by epifluorescence (*Fpn-GFP*) and immunostaining (*Cp*). *DIC*, differential interference contrast. *B,* C6 cells were silenced for Cp-GPI and co-transfected with Fpn-GFP and hCp-GPI R701W or Q692K. Dominance of the mutation was assessed by further co-transfection with hCp-GPI WT. Cells were examined after 24 h by epifluorescence (*Fpn-GFP*) and immunostaining (*Cp*). *C,* C6 cells were silenced for Cp-GPI and co-transfected with Fpn-GFP, hCp-GPI R701W, and secreted hCp WT. Cells were examined by epifluorescence (*Fpn-GFP*) and immunostaining (*Cp*) after 24 h in the absence or presence of 50 μM Cu(I)-GSH complex in the medium. The corresponding culture supernatants were concentrated and analyzed by nondenaturing SDS-PAGE and Western blot to distinguish apo- and holo-Cp. Quite similar results were obtained when secreted hCp R701W and hCp-GPI WT were employed.

SUBSTITUTION OF ARGININE 701 WITH TRYPTOPHAN IMPAIRS ATP7B-DEPENDENT COPPER LOADING PROCESS AND CAUSES GOLGI APPARATUS FRAGMENTATION

When secreted hCp WT and R701W were expressed in the yeast *P. pastoris* and partially purified from culture medium, they both showed robust oxidase activity, as shown by non-denaturing SDS and staining with o-dianisidine (Fig. 4A, left panel). This indicates that both hCp WT and R701W can be obtained as holo-proteins by heterologous expression in yeast.

The recombinant proteins were hyperglycosylated, as demonstrated by the electrophoretic shift observed after treatment with endoH (Fig. 4A, right panel). The right panel of Fig. 4A was run under denaturing conditions, and therefore the electrophoretic mobilities cannot match those observed in the left panel. Addition of the recombinant proteins produced in yeast, either WT or R701W, to the medium of C6 cells silenced for Cp-GPI completely rescued Fpn-GFP (Fig. 4B), unequivocally indicating that oxidase-active hCp R701W is functional and that the ferroxidase activity of Cp is sufficient to stabilize Fpn.

Consistently, iron scavenging from Fpn by addition of either purified native hCp, purified yeast ferroxidase Fet3p, or the iron chelator BPS (De Domenico et al., 2007) to cells silenced for endogenous Cp- GPI and transfected with hCp-GPI R701W stabilized Fpn at the plasma membrane (Fig. 5), also confirming that hCp-GPI R701W on the plasma membrane does not per se impair Fpn or hCp WT.

Copper loading of hCp R701W can thus take place efficiently in yeast, but it is critically perturbed in mammalian cells with a dominant effect over co-expressed hCp WT. Copper delivery in the secretory pathway requires the copper-transporting ATPases ATP7A and ATP7B in mammalian cells (Lutsenko et al., 2007) and their homologue Ccc2p in yeast (Yuan et al., 1995).

Studies on the biosynthesis of Cp demonstrate that the protein acquires copper from ATP7B in the secretory pathway in an “all-or-none” process (Lutsenko et al., 2007, Kono et al., 2007 and references therein). Co-expression of *S. cerevisiae* Ccc2p in C6 cells transfected with hCp-GPI R701W revealed that Fpn-GFP was very reproducibly rescued in about 30% of the cells (Fig. 4C). Similar results were obtained on C6 cells silenced for ATP7B and co-transfected with *S. cerevisiae* Ccc2p and hCp-GPI WT or hCp-GPI R701W (data not shown).

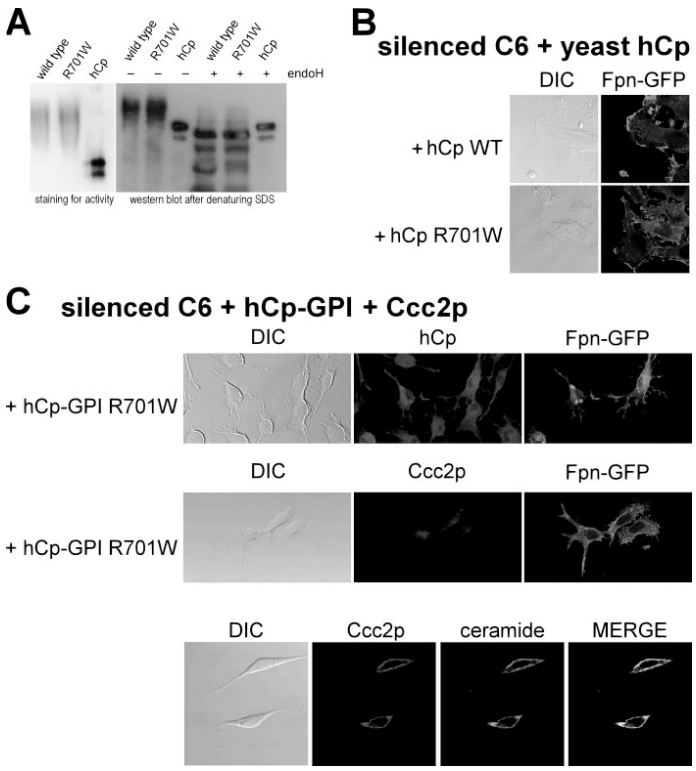

Figure 4. Copper incorporation in hCp R701W is promoted by yeast Ccc2p. *A,* secreted human Cp WT and R701W produced in yeast were partially purified by anion exchange chromatography on DEAE-Sephacel and analyzed by nondenaturing SDS-PAGE and staining for oxidase activity with *o*-dianisidine (*left panel*) or by Western blot in denaturing conditions before and after deglycosylation by endoH (*right panel*). *B,* cells were silenced for Cp-GPI, transfected with Fpn-GFP, and recombinant secreted human Cp WT or R701W (0.1 μM) produced in the yeast *P. pastoris* was added to the medium. After 24 h cells were examined by epifluorescence. *DIC,* differential interference contrast. *C, upper* and *middle panels,* cells silenced for Cp-GPI were transfected with Fpn-GFP, human Cp-GPI R701W, and *S. cerevisiae* Ccc2p-FLAG. After 24 h cells were examined by epifluorescence (*Fpn-GFP*) and immunostaining (*Cp, Ccc2p*). *Lower panel,* cells transfected with *S. cerevisiae* Ccc2p-FLAG were stained with NBD-C6-ceramide and observed by epifluorescence (Golgi) and immunostaining (Ccc2p).

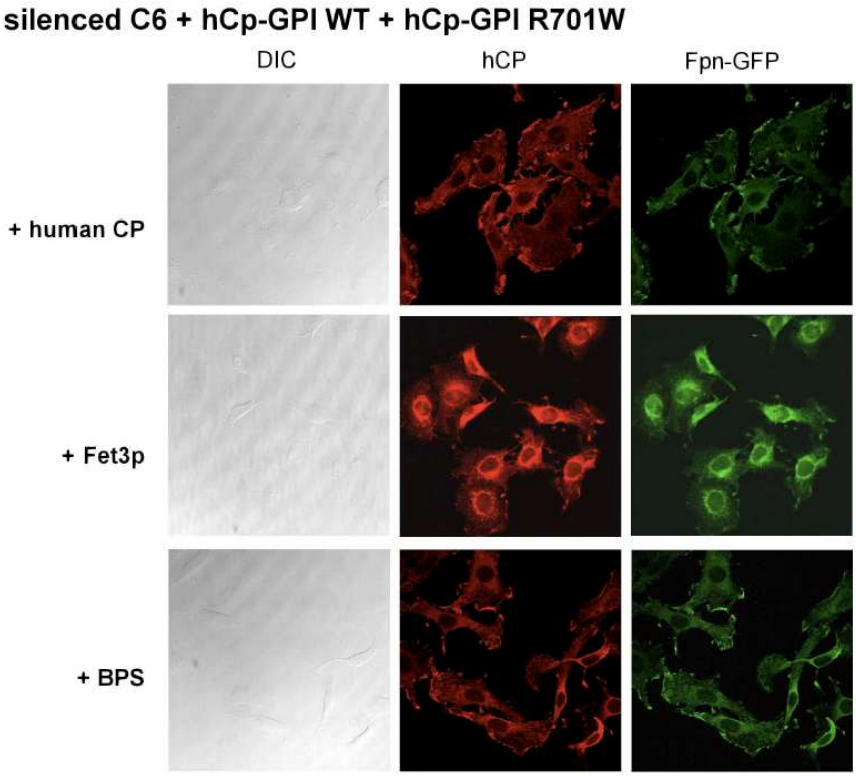

Figure 5. Scavenging of extracellular Fe(II) rescues Fpn-GFP in the presence of Cp R701W. Cells silenced for Cp-GPI were transfected with Fpn-GFP and hCp-GPI WT and R701W. Purified hCp (1 µM), purified secreted *P. pastoris* Fet3p (1 µM) or the iron chelator BPS (200 µM) was added to the medium and cells were examined after 24 h by epifluorescence (Fpn-GFP) and immunostaining (Cp). Secreted *P. pastoris* Fet3p truncated at residue 552 was expressed in the fet3Δ *P. pastoris* strain using the pIB2 vector; yeast cells were grown in 1 lt minimal medium buffered at pH 6 with 50 mM potassium phosphate, supplemented with 100 µM $CuSO_4$ and harvested at OD_{600} 2-3. The culture supernatant was filtered, brought to pH 7.4 and loaded on DEAE-Sephacell (10 ml resin) equilibrated in 25 mM MOPS pH 7.4, 120 mM NaCl. Fet3p was eluted at 300 mM NaCl, SDS-PAGE analysis demonstrated that the protein was >90% pure with a yield of about 1 mg.

These findings indicate that the *S. cerevisiae* copper transporter can directly, although partially, complement the defect caused by hCp R701W on the mammalian copper-ATPase and that the efficiency of copper delivery is about

equal for the WT and the mutant protein.

The middle panel of Fig. 4C focalizes on cells where Fpn was rescued by overexpression of Ccc2p in the presence of hCp R701W. As expected, cells where Fpn was rescued were positive for Ccc2p, and the yeast ATPase displayed a diffuse perinuclear staining suggestive of localization in the Golgi compartment. The focal plane was in this case chosen to maximize the observation of Fpn-GFP.

The localization of Ccc2p was unequivocally demonstrated by using NBD-C6-ceramide, a well-established Golgi marker. As shown in the bottom panel of Fig. 4C, Ccc2p completely co-localized with ceramide. In this case, focusing was set across the nuclear plane, and the perinuclear localization of the ATPase is much more evident. Ccc2 was also found to co-localize with both the trans-Golgi TGN-38 and the cis-Golgi GM130 (data not shown).

The dominant negative effect of hCp R701W could then be due to abnormal interaction of the transporter with the ferroxidase, which could possibly make ATP7B unavailable even for hCp WT. However, attempts to co-immunoprecipitate hCp-GPI WT or R701W with ATP7B were unsuccessful. This could be due to inefficient capturing by the polyclonal antibody or to disruption of the interaction in the experimental conditions imposed on the lysates.

Therefore, the subcellular localization of ATP7B was directly assessed by immunofluorescence. For this experiment, hCp-GPI tagged with the FLAG epitope was employed to allow use of different conjugated secondary antibodies (i.e. anti-mouse versus the monoclonal anti-tag antibodies and anti-rabbit versus anti-ATP7A/B) for simultaneous visualization of both proteins. The analysis showed that ATP7B is expressed in C6 cells with a diffuse perinuclear staining and that the subcellular localization of the transporter is unaffected by transfection with hCp-GPI WT (Fig. 6). Silencing of endogenous Cp did not affect ATP7B localization as well (data not shown). On the other hand, ATP7B partially relocates to more peripheral vesicular compartments in cells expressing hCp-GPI R701W (Fig. 6). At variance with what was observed with hCp-GPI WT, merging of ATP7B and hCp-GPI R701W immunofluorescence was apparently significant, suggesting a stronger interaction with the transporter in the latter case. Higher magnification images of the subcellular localization of ATP7B are shown in Fig. 6B. Here, cells silenced for endogenous Cp and transfected with either hCp-GPI WT or R701W were stained for both the trans-Golgi network marker TGN-38 and ATP7B. The merged fields show that the

ATPase invariably co-localizes with the trans-Golgi network marker, and that the presence of the mutant protein apparently induces a significant fragmentation of the Golgi apparatus and the formation of vesicles originating from the trans-Golgi network itself (Fig. 6B).

All the other aceruloplasminemia Cp mutants were not dominant when co-expressed with Cp WT, and they did not induce a change in localization of ATP7B, irrespective of their ability to bind copper.

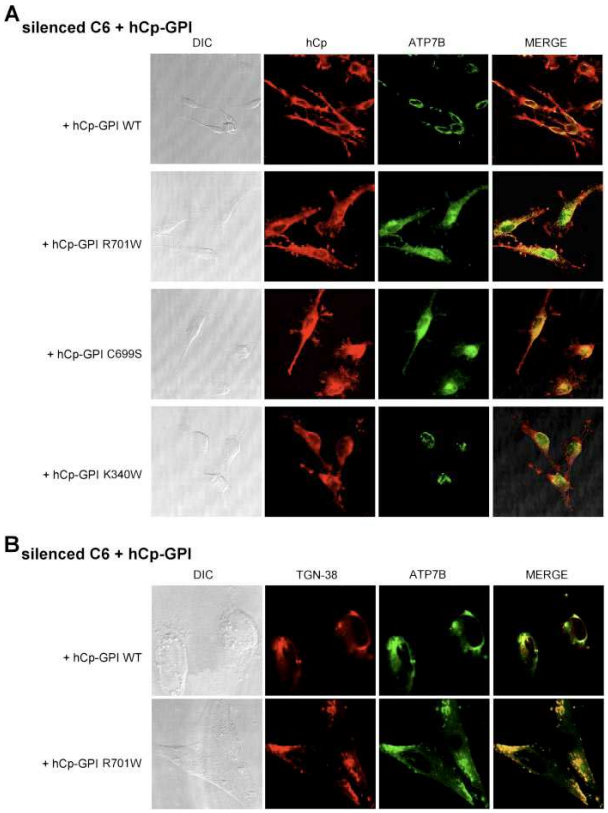

Figure 6. Human Cp-GPI R701W and C699S induce relocalization of ATP7B. *A,* cells silenced for Cp-GPI were transfected with FLAG-tagged human Cp-GPI WT or mutant, as indicated, and immunostained for the FLAG tag and for ATP7B. *B,* higher magnification images of cells silenced for Cp-GPI, transfected with human Cp-GPI WT or R701W, and immunostained for TGN-38 and ATP7B. *DIC,* differential interference contrast.

Possible role of solvent-exposed loops in aceruloplasminemia

To gain further insight on the origin of the defect carried by hCp R701W, the structure of the protein was analyzed. Cp is a multidomain protein made up of six plastocyanin-like domains with ternary pseudosymmetry (Fig. 7).

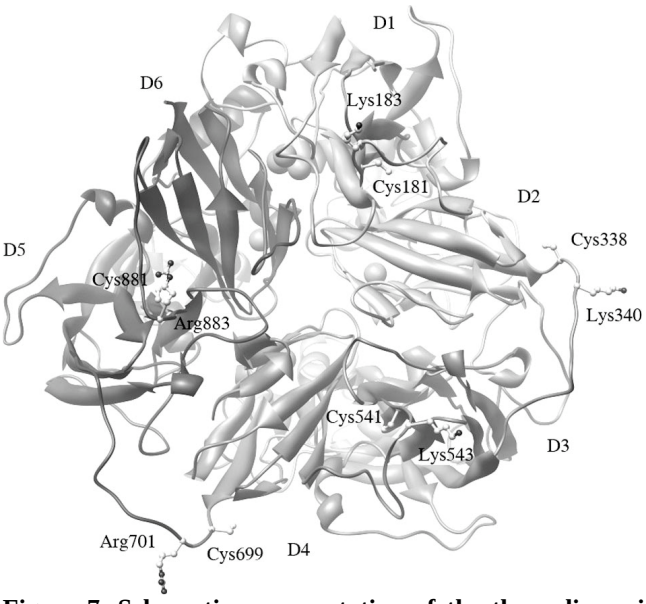

Figure 7. Schematic representation of the three-dimensional structure of Cp. For clarity, only the residues making up the Cys-*X*-(Arg/Lys) motifs located on the loops connecting Cp domains (Cys-181 and Lys-183, Cys-338 and Lys-340, Cys-541 and Lys-543, Cys-699 and Arg-701, Cys-881 and Arg-883) are shown in *ball-and-stick* representation. Copper ions are indicated by *spheres*. Domains 1 and 2, 3 and 4, 5 and 6 are light grey, grey, and dark grey respectively and indicated by the labels *D1–D6*. The figure was produced with Chimera.

Domains 1 and 2, 3 and 4, and 5 and 6 interact with each other through extensive, highly packed hydrophobic interfaces, whereas polar interactions and loosely packed interfaces are present between domains 2 and 3 and 4 and 5, with the interface between domains 6 and 1 hosting the catalytically essential trinuclear copper cluster. Residue Arg-701 is located in a large solvent-exposed loop connecting domains 4 and 5 and comprising residues 700–708; a corresponding loop which connects domains 2 and 3 is found at positions 339–

350. Domains held together by hydrophobic interactions are also connected by surface loops. Despite a low degree of sequence homology, all these loops start with a CX(R/K) motif, with the cysteine residue stabilizing the loop by forming a disulfide bridge. The position of the five loops and the identity of the basic residue within the CX(R/K) motif are also shown in Fig. 7.

The role of the 700–708 loop was investigated by extensive mutagenesis. Residue Arg-701 was either deleted or substituted with glutamine (R701Q), glutamic acid (R701E), or phenylalanine (R701F) to test whether it is specifically the bulky hydrophobic tryptophan side chain that gives rise to a nonfunctional Cp or any substitution at position 701 is deleterious.

Mutants R701Δ, R701Q, R701E, and R701F were unable to rescue Fpn-GFP, yet they were not dominant and did not result in relocalization of ATP7B (Fig. 8).

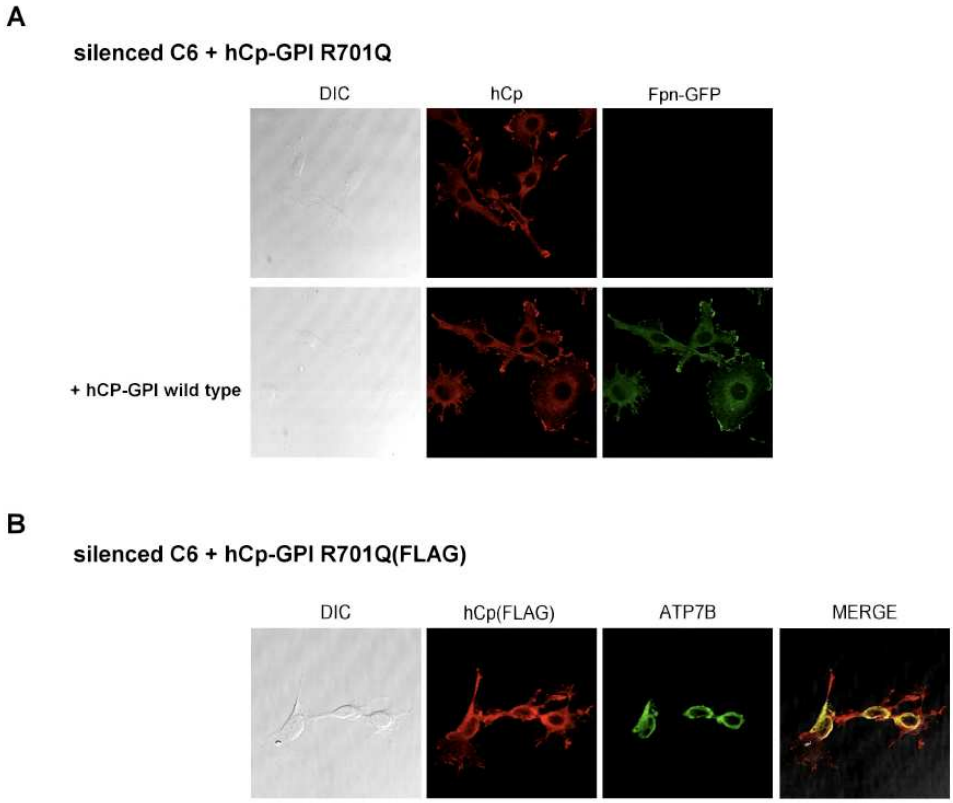

Figure 8. Human Cp R701Q, R701E and R701Δ are non functional, not dominant, and do not impair ATP7B localization. The figure representatively shows the case of hCp R701Q. A) Cells silenced for Cp-GPI were transfected with Fpn-GFP and hCp-GPI R701Q in the presence or absence of hCp-GPI WT. Cells were examined by epifluorescence (Fpn-GFP) and immunostaining (Cp). B) Cells silenced for Cp-GPI were transfected with FLAG-tagged hCp-GPI R701Q and immunostained for the FLAG tag and for ATP7B.

Mutants Q702M, S703A, E704M, and D705M were functional and rescued Fpn-GFP in Cp-GPI silenced cells, whereas substitutions that were definitely non-conservative and structurally more challenging (R700W, Q702W, E704W, and D705P) yielded proteins unable to complement the loss of endogenous Cp; all proteins were localized at the plasma membrane, and the inactive mutants were not dominant.

The possible role of other loops in copper incorporation into hCp was tested by replacing the basic residues corresponding to Arg-701 with tryptophan. The Cp mutants were expressed in yeast while their ability to maintain Fpn-GFP on the plasma membrane was assessed by transfection in mammalian cells silenced for endogenous Cp-GPI. All Arg/Lys→Trp mutants (K183W, K340W, K543W and R883W) were non-functional in mammalian cells (representatively shown for K543W in Fig. 9), but at variance with the R701W mutant, they did not show the dominant negative effect over wild type Cp, and did not affect Golgi morphology (data not shown), suggesting a peculiar role for the Arg701-containing loop.

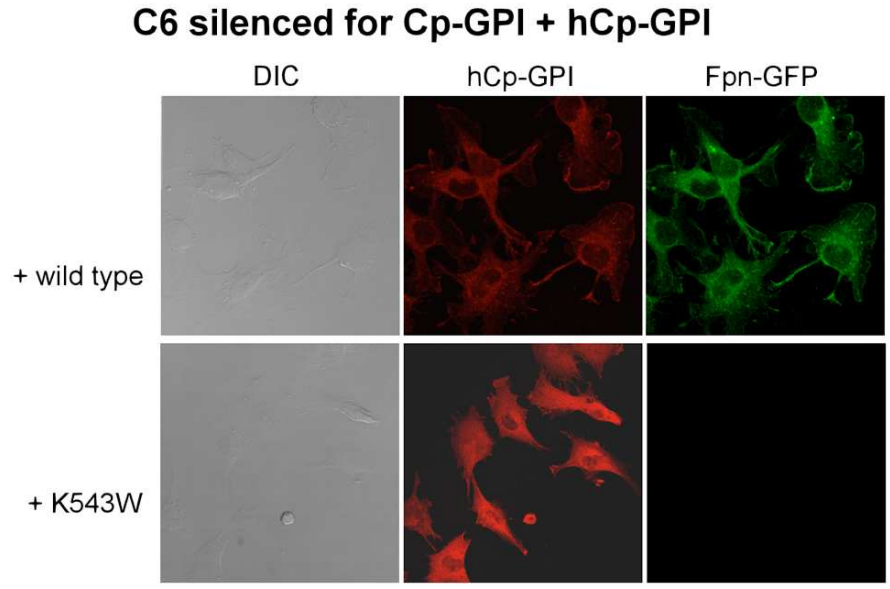

Figure 9. Cp mutant K543W is unable to rescue Fpn-GFP in C6 silenced for endogenous ceruloplasmin. Rat glioma C6 cells were silenced for Cp-GPI. After 24 h they were transfected with Fpn-GFP and human Cp-GPI K543W. Cells were analyzed after 24 h by epifluorescence (Fpn-GFP) and immunostaining (hCp). *DIC*, differential interference contrast.

However, they showed oxidase activity when expressed and partially purified in yeast (Fig. 10 and Table 1). Specific oxidase activity was similar to wild type Cp, ranging from about 70% to 100% for the different mutants. These results indicate that mutation of the basic residue of all loops dramatically

interferes with proper copper loading of Cp in mammalian cells, but not in yeast.

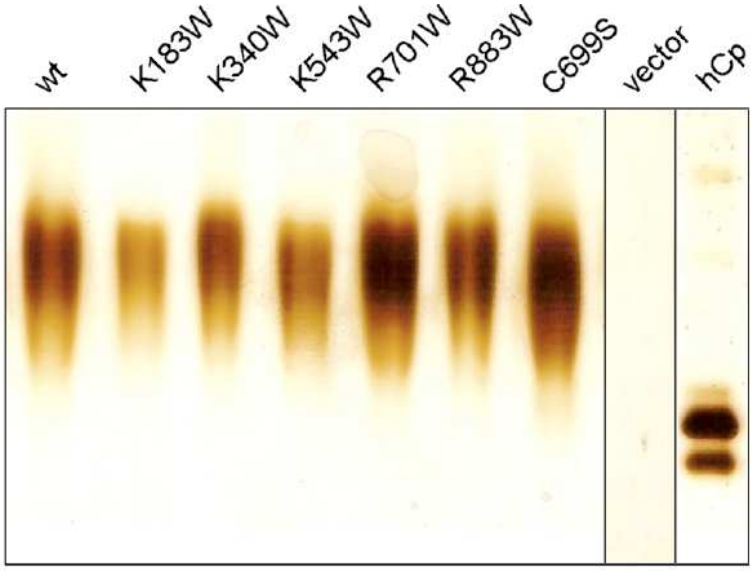

Figure 10. Non-denaturing SDS-PAGE analysis of oxidase activity of recombinant wild type and mutant Cp. Approximately three μg total protein were loaded per lane and the gel was stained with o-dianisidine. Transfected empty vector was used as negative control. Note the lower electrophoretic mobility of the recombinant proteins compared to hCp, due to hyperglycosylation.

Table 1. Enzymatic and functional activity of human Cp expressed in *P. pastoris.*

Ceruloplasmin	Oxidase activity[a]	Specific activity	Functional complementation[b]
Wild Type	0.078	100	+++
R701W	0.053	68	- D
K183W	0.071	91	-
K340W	0.075	96	-
K543W	0.077	99	-
R883W	0.052	67	-
C699S	0.062	79	- D
C618S	0.034	44	- D

[a] ΔA_{540}/h/µg Cp at 37°C pH 6 (blank: sample boiled 5').
[b] Functional complementation in C6 cells silenced for endogenous Cp-GPI and co-transfected with Fpn-GFP and the corresponding Cp mutant. D: dominant over wild type Cp.

To further explore the role of the loops in the process of copper incorporation, the disulphide bridge preceding the basic residues was disrupted by substituting the cysteine residues with serine. Cp mutants C181S, C257S, C338S and C541S were unable to rescue Fpn-GFP unless yeast Ccc2p was co-expressed in C6 cells, as representatively shown for C541S (Fig. 11).

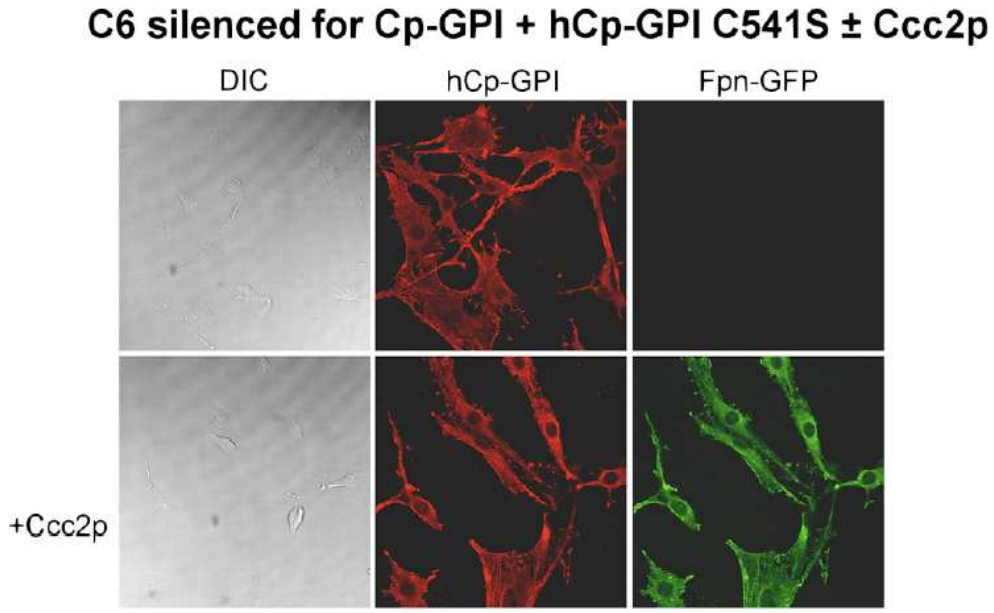

Figure 11. Analysis of complementation by Cp-GPI C541S of endogenous Cp silencing in C6 cells. Rat glioma C6 cells were silenced for Cp-GPI. After 24 h they were transfected with Fpn-GFP and human Cp-GPI C541S. Yeast ATPase Ccc2p ability to deliver copper to the mutant Cp was assessed by further co-transfection with recombinant *P. pastoris* Ccc2p-Flag. Cells were analyzed after 24 h by epifluorescence (Fpn-GFP) or immunofluorescence (hCp).

These mutants were not dominant over wild type Cp and Golgi morphology was normal. Interestingly, in these experiments we used *P. pastoris* Ccc2p, which appeared to be more efficient than its homolog from *S. cerevisiae*, with cell-surface Fpn-GFP present in practically all cells compared to about 30% of the cells obtained by co-transfections with *S. cerevisiae* Ccc2p (see Fig. 4). This is not due to different transfection efficiencies and/or expression levels of the ATPases, as demonstrated by Western blot analysis (Fig. 12).

Figure 12. Expression of yeast Ccc2p. Western blot analysis of recombinant Flag-tagged *S. cerevisiae* Ccc2p and *P. pastoris* Ccc2p expressed in C6 cells. Equal loading was confirmed by staining with Ponceau S.

Disruption of the disulphide bridge of the R701 loop was much more devastating because both mutants C699S and C618S exhibited the same phenotype of R701W: they were non-functional, dominant over wild type Cp and they induced fragmentation/dispersal of the Golgi apparatus (Fig 6 for C699S and Fig. 13 for C618S).

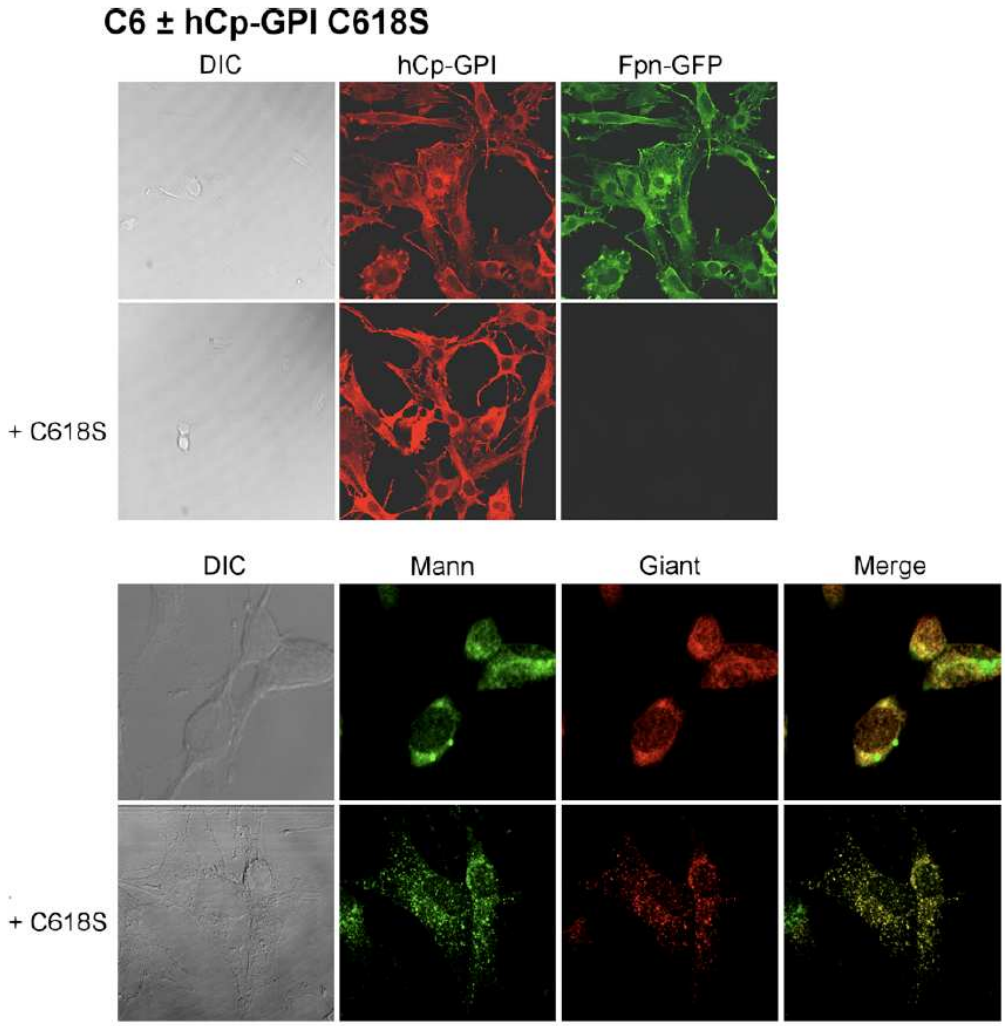

Figure 13. Human Cp-GPI C618S is dominant over wild type CP and induces dispersal of the Golgi apparatus. Upper panel: Rat glioma C6 cells were transfected with Fpn-GFP and, when indicated, with hCp-GPI C618S. After 24 h they were analyzed by epifluorescence (Fpn-GFP) or immunofluorescence (hCp). Lower panel: higher magnification images of C6 non transfected or transfected with Cp-GPI C618S and immunostained for Golgi markers (mannosidase, Mann and giantin, Giant).

Specific Golgi markers were used to show that vesicles formed in the presence of mutant C618S originated from the Golgi apparatus. As shown in Fig. 13, lower panel, in untransfected cells mannosidase II co-localized with the Golgi matrix protein giantin, yielding the expected perinuclear localization. When cells were transfected with hCp-GPI C618S both Golgi markers appeared to be redistributed from the typical ribbon pattern to a vesicular haze extensively dispersed throughout the cytosol. Identical results were obtained with hCp-GPI C699S. Co-expression with Ccc2p rescued Fpn-GFP, even though the Golgi was dispersed (Fig. 14).

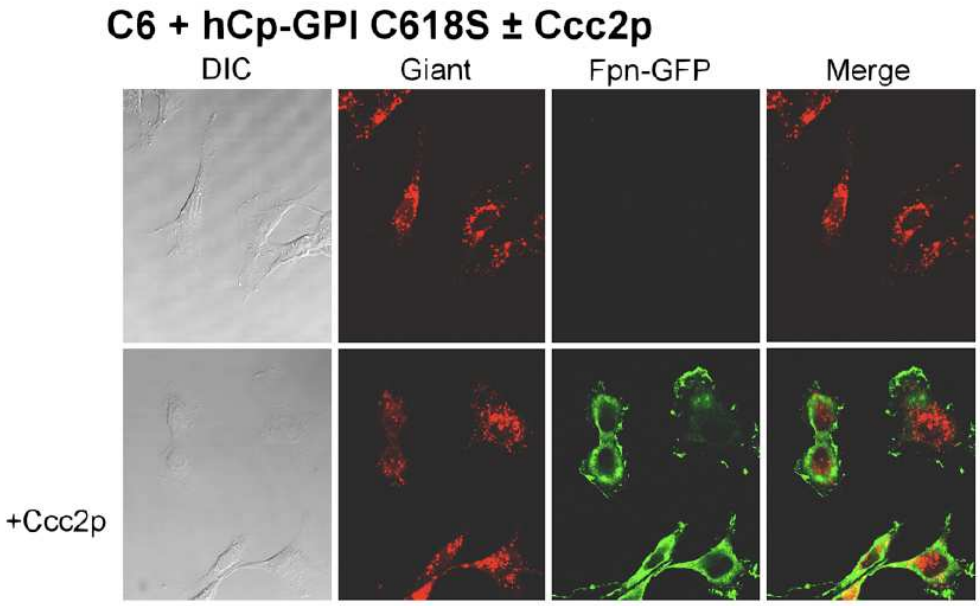

Figure 14. Yeast Ccc2p can reverse the effect of Cp-GPI C618S. Rat glioma C6 cells were transfected with Fpn-GFP and with hCp-GPI C618S. After 24 h they were analyzed by epifluorescence (Fpn-GFP) or immunofluorescence (hCp). Co-transfection with *P. pastoris* Ccc2p rescues Fpn-GFP even though Golgi still appears fragmented.

Both C618S and C699S mutants were found to be catalytically active when expressed in yeast , with 44% and 79% activity respectively relative to wild type (Table 1), indicating that mutation of the cysteines did not induce gross folding defects. Thus, Cp mutations R701W, C699S and C618S all appear to

interfere with Golgi morphology and copper loading selectively in mammalian cells.

Golgi dispersal could be due to abnormal interaction of mutant Cp and ATP7B with consequent inactivation of the ATPase or to some other (more or less independent) phenomenon triggered by mutant Cp. A possible way of discriminating between the two hypotheses is to silence ATP7B in cells expressing Cp-GPI R701W and to analyze Golgi status. Results obtained indicate that the Golgi is dispersed in C6 cells silenced for ATP7B and transfected with Cp-GPI R701W (Fig. 15), suggesting that it is an intrinsic property of the mutant Cp that gives rise to the changes in Golgi morphology.

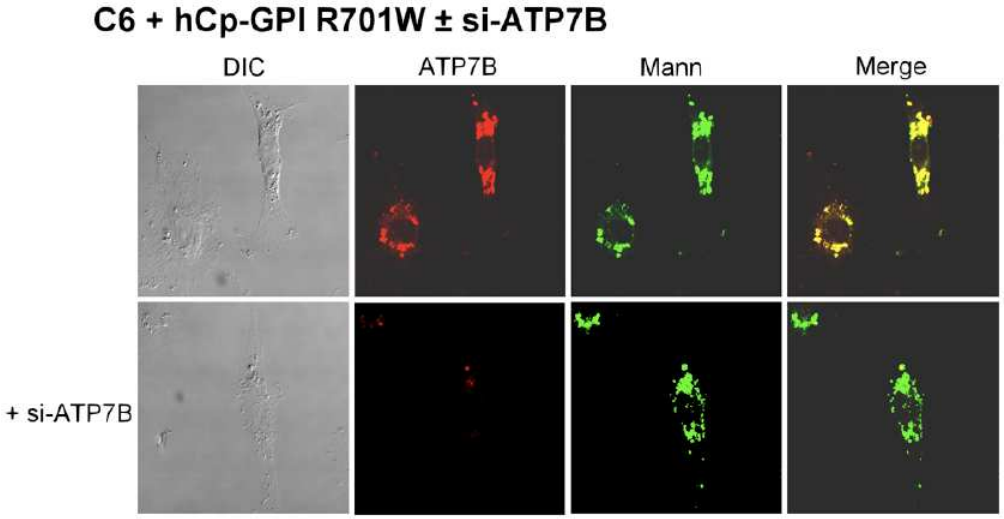

Figure 15. Golgi is fragmented in C6 silenced for ATP7B and transfected with Cp-GPI R701W. Cells were silenced for ATP7B when indicated and then transfected with Cp-GPI R701W. After 24 h they were examined by immunostaining for ATP7B and mannosidase (Mann).

CP R701W CAUSES STRONG INTRACELLULAR OXIDATIVE STRESS. GOLGI APPARATUS FRAGMENTATION CAN BE PREVENTED BY REACTIVE OXYGEN SPECIES SCAVENGERS GLUTATHIONE AND N-ACETYL-CYSTEINE

The disassembly of the Golgi apparatus as well as chronic oxidative stress and accumulation of metals (e.g., iron and copper), are frequently associated with the pathogenesis of several neurodegenerative disorders. Therefore, we investigated the level of reactive oxygen species (ROS) production in C6 cells expressing the Cp mutant R701W. To assess the formation of intracellular ROS we used the fluorescent dye H_2DCFDA. As shown in Fig. 16A, ROS levels were significantly increased in C6 cells expressing Cp R701W at 24 h post-transfection. In particular, we found that intracellular ROS have a specific punctate distribution inside the cells, partially localized at the lysosomal compartment, as appears by double-staining with lysotracker dye in Fig. 16B. Moreover, lysosome distribution and total lysosome number into the cells appear to be increased.

To determine whether ROS production was affected by ROS scavengers, cells were pre-treated with well-known antioxidants, NAC or GSH, for all the time of transfection up to 24 h. Pre-treatment with 2 mM NAC or GSH significantly reduced the intracellular ROS levels as shown in Fig. 16C.

To verify the involvement of ROS in Cp R701W-induced Golgi apparatus fragmentation and ferroportin degradation we performed experiments on transfected C6 cells pre-treated with 2 mM NAC or GSH and analyzed the Golgi morphology and the presence of ferroportin at the plasma membrane. Fig. 17 shows that both NAC and GSH were able to completely restore Golgi morphology, as demonstrated by the staining with anti-giantin antibody. Moreover, scavenging of ROS by NAC or GSH prevented ferroportin degradation as shown in Fig. 17. These findings clearly indicate a role for ROS in this pathway.

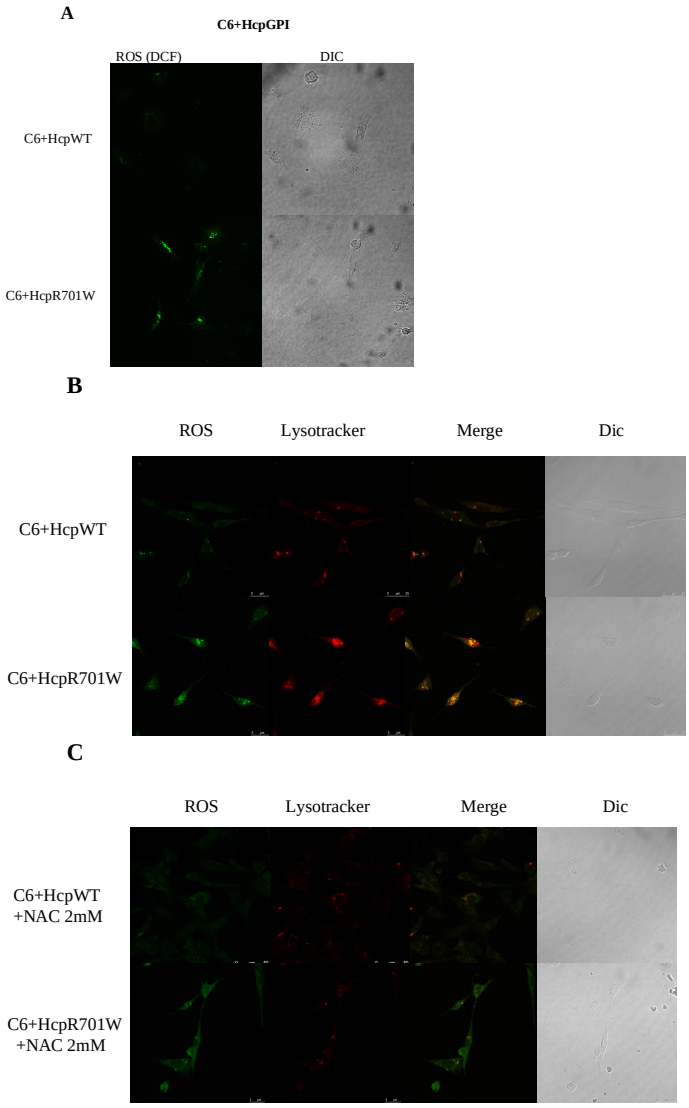

Figure 16. Cp R701W causes production of ROS. A-B) Rat glioma C6 cells were transfected with hCp WT or R701W, ROS and lyososome staining and visualization were performed 24 h after trasfection. C) Rat glioma C6 cells were transfected with FpnGFP and hCp WT or R701W, lysosome staining with lysotracker and epifluorescence microscopy were performed 24 h after transfection.

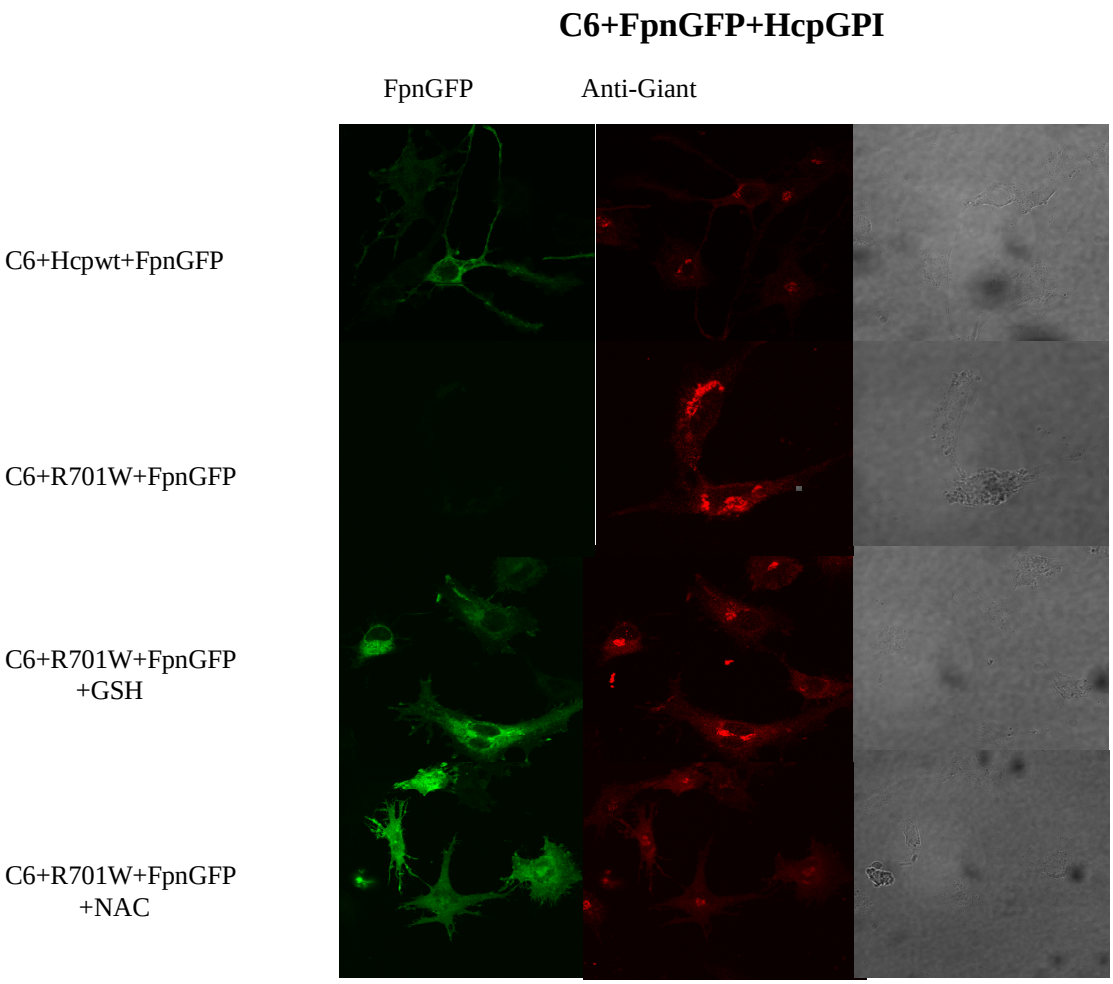

Figure 17. NAC and GSH prevent Golgi fragmentation. Rat glioma C6 cells were transfected with Fpn-GFP and hCp-GPI WT or R701W. NAC 2 mM or GSH 2 mM were added in the media and in the transfection mix. Immunofluorescence with anti-Giantin was performed to visualize Golgi status 24 h after transfection.

DISCUSSION

Aceruloplasminemia is generally associated with complete absence of serum Cp because of homozygous mutations of the Cp gene, although some patients are heterozygous for the causative mutation. The few disease-associated mutants that had been characterized up to now invariably lacked ferroxidase activity and fall into one of two categories as follows: truncated mutants are generally retained in the ER and cause ER-associated stress and activation of the 'unfolded protein stress response' (Kono et al., 2006, Kono et al., 2007); missense mutants display a folding defect that leads to retention in the ER (I9F and P177R) or they are secreted as apo-proteins (G631R and G969S). Residues Gly-631 and Gly-969 are close to type 1 copper sites in domains 4 and 6, and their substitution introduces a structural defect that makes the protein unable to bind copper, as also demonstrated by the finding that it cannot be reconstituted by copper in vitro (Hellman et al., 2002, Kono et al., 2006). Apo-Cp is unstable, and it is degraded in serum with a half-life of hours compared with days for the holo-protein (Holtzman and Gaumnitz, 1970), explaining the failure to detect Cp in the serum of patients.

The simplest model links the iron overload observed in the brain of aceruloplasminemia patients to lack of a ferroxidase-active Cp-GPI on the plasma membrane of astrocytes. In line with this model, inactive mutants P177R, G631R, and G969S are unable to prevent the internalization and degradation of Fpn in C6 cells silenced for Cp-GPI. Also mutant Q692K is nonfunctional. This is not surprising because Gln-692 located close to Met-690, a type 1 copper ligand in domain 4, in a highly conserved region sandwiched between Lys-691 and Lys-693 and oriented toward the protein interior. Thus, all these mutations affect the ability of Cp to bind copper.

A novel mechanism causing aceruloplasminemia is defined by mutations on Cp that do not abrogate the ability of the protein to bind copper but impair the copper loading process requiring the copper-ATPase ATP7B. Mutants D58H and R701W are secreted as apo-proteins, but at variance with all other missense aceruloplasminemia mutants, they can be reconstituted by the Cu(I)-GSH complex. This complex seems to exert a general stabilizing effect on secreted Cp, as higher quantities of the protein are present in the medium of cells transfected with any mutant and treated with Cu(I)-GSH. The alternative hypothesis that Cu(I)-GSH enhances secretion of hCp cannot be ruled out at this

stage; however, it should be reminded that Cp can bind extra copper ions besides the canonical six metal atoms, and that these extra ions could help to slow down protein degradation.

Our findings can be taken as an indication that the intracellular copper loading process is disturbed by some Cp mutants. Data in support of this hypothesis include the functional complementation afforded by externally added holo-Cp WT or R701W produced in yeast and the recovery of Fpn-GFP in the presence of Cp R701W if the missense Cp mutant is co-expressed with the yeast copper transporter Ccc2p. Misfunctioning of the copper loading process is accompanied by a gross rearrangement of the Golgi apparatus, which appears fragmented in the presence of Cp R701W.

Expression in yeast can offer information on the intrinsic capacity of the Cp mutants to bind copper. As a matter of fact, all mutants that were inactive in the functional complementation assay were also enzymatically inactive when produced in yeast. Only Cp R701W and the 'loop mutants' (C618S, C699S, K183W, K340W, K543W and R883W) were active in yeast and inactive in mammalian cells. Our data indicate that this is because of impairment of the copper-loading process involving the mammalian copper-transporting ATPase ATP7B.

The mechanism of coupling between copper transport and copper incorporation into target proteins is not understood, although it does not seem to involve additional proteins (El Meskini et al., 2007). Precise fit of the transporter and acceptor protein is probably not essential for copper delivery, because the mammalian copper-ATPases can load the yeast multicopper oxidase Fet3p (Hsi et al., 2008, Hung et al., 1997), and vice versa the yeast transporter Ccc2p can deliver copper to human Cp, although efficiency is lower in both cases.

In this respect, it is both intriguing and puzzling that the efficiency of rescue of Fpn is partial with Cu(I)-GSH or Ccc2p (i.e. only some cells show the presence of Fpn-GFP, although all cells are exposed to hCp reconstituted by Cu(I)-GSH), as if the amount of holo-Cp produced must reach a cell-specific threshold to produce functional complementation.

In the six-domain structure of Cp, K183, K340, K543, R701 and R883 are located in long surface loops which connect the various domains. A central observation is that disruption of the native structure of the external loops of Cp is not per se sufficient to prevent the ATPase-assisted copper loading (yeast Ccc2p is able to deliver copper to Cp). A possible explanation is that a conformational rearrangement of Cp is required for proper copper loading, and that mutation of

the basic residues on the loops, or disruption of the preceding disulphide bridges, impairs the conformational rearrangement by anomalously increasing the affinity between Cp and ATP7B (but not Ccc2p). For instance, ‘closure’ of domains 5 and 6 onto domain 1 could be necessary for delivery of copper to take place onto the trinuclear copper cluster (whose ligands are indeed provided by both domains 6 and 1). Since the loops are located in a flat region at the bottom of the Cp structure, it is tempting to speculate that this region be responsible for improper interaction with ATP7B when the native loop structure is destroyed. This model would be consistent with the topology of ATP7B, which places the metal binding domains on the cytosolic side of the membrane and predicts exit of copper from the transmembrane channel into the lumen.

Mutation R701W, however, is peculiar in that it exerts a dominant negative effect that appears to go beyond the simple impairment of the ATPase.

Disruption of the disulfide bridge Cys-618 to Cys-699 preceding Arg-701 by replacement of Cys-618 or Cys-699 with serine also generates dominant Cp mutants, highlighting the importance of this loop. Cp R701W, C699S or C618S appear to cause a change in localization of the ATPase and ‘functional silencing’ of ATP7B. We use this term not to imply that ATP7B is necessarily dysfunctional, but simply to indicate that the ATPase is not ready for copper delivery to Cp. Indeed, in the presence of either Cp C618S, Cp C699S or Cp R701W a significant dispersal of the Golgi apparatus takes place. In this respect, relocalization of ATP7B could be part of a general phenomenon involving most of the secretory compartment. The observed redistribution of TGN-38 and mannosidase II implies that the mutant Cp R701W has much more global effects in the cell than just the mislocalization of ATP7B and thus is doing more than impairing the copper loading machinery.

However, as far as Fpn rescue is concerned, the ability of the yeast pump Ccc2p to load copper into Cp R701W indicates that, despite the general effect on the Golgi apparatus, Cp R701W retains the ability to acquire copper under proper conditions and, in turn, to prevent degradation of Fpn that would occur in the absence of the oxidase.

Fragmentation of the Golgi apparatus appears to be a general hallmark of neurodegenerative disease. Examinations of human brain tissues and animal models have shown that fragmentation of the Golgi apparatus is found in Alzheimer disease, amyotrophic lateral sclerosis, Creutzfeldt-Jacob disease, multiple system atrophy, Parkinson disease, spinocerebellar ataxia type 2, and

Niemann-Pick disease type C. This has led to the hypothesis that the morphological status of the Golgi apparatus may be a reliable index of activity of degeneration (Stieber et al., 1996).

There is increasing evidence that the lysosome is also involved in the pathogenesis of a variety of neurodegenerative diseases, including Alzheimer's disease, Parkinson's disease, Huntington's disease, and amyotrophic lateral sclerosis. Abnormal protein degradation and deposition induced by lysosomal dysfunction may be the primary contributor to age-related neurodegeneration (Zhang et al., 2009).

In this context, it is not surprising that the mutation R701W, which causes severe neurological symptoms, can induce fragmentation of the Golgi apparatus. From a molecular point of view, it is difficult at this stage to explain how a single amino acid substitution on Cp might lead to the dramatic effect observed on the Golgi apparatus.

This observation, however, is not unprecedented. Some mutations of superoxide dismutase that are involved in the onset of familial amyotrophic lateral sclerosis are associated with fragmentation of the Golgi apparatus in spinal cord motor neurons (Fujita et al., 2000, Stieber et al., 2004).

Although the molecular mechanism still awaits to be unraveled, it is clear that interactions between mutant proteins and any of one or more proteins involved in the maintenance of the structure of the Golgi apparatus might interfere with its structure and function (Gonatas et al., 2006). In this respect, the finding that Cp R701W induces strong and localized production of ROS can link the effect on Golgi to neurodegeneration.

It is well known that ATP7B changes its subcellular distribution depending on copper availability (Lutsenko et al., 2007); however, copper does not induce fragmentation of the Golgi apparatus. Moreover, the fact that Cp mutants that do not bind copper (such as G631R or Q692K) do not induce relocalization of ATP7B seems to exclude that an increase in the local copper concentration is responsible for this phenomenon. Lack of ATP7B cannot be fully compensated by ATP7A in many tissues that express both proteins (Lutsenko et al., 2007). This appears to be true also for glioma cells, suggesting that Cp-GPI expressed in astrocytes is strongly dependent on ATP7B for acquisition of copper.

We believe that failure to incorporate copper in WT Cp together with aberrant localization of ATP7B and significant fragmentation of the Golgi apparatus induced by oxidative stress are critical determinants of the severity of

the phenotype observed in the heterozygous patient carrying the Cp R701W mutation.

It is worth noting that R701W is the only mutation known so far that leads to severe neurological symptoms at a young age, despite the heterozygous genotype with the presence of the WT allele (Kuhn et al., 2005). It should be added that the father of this patient is also heterozygous for the R701W mutation, yet he is asymptomatic (Kuhn et al., 2005). This is consistent with our observation that the R701W mutation can be overcome under proper conditions (e.g. through increased extracellular copper bioavailability or in the presence of ROS scavengers), and suggests that the severity of some forms of aceruloplasminemia is probably modulated by modifier genes and/or metabolic status. In addition, the molecular analysis of ATP7B could provide additional information, e.g. specific isoforms of the ATPase might be responsible for the different phenotypes.

Asp-58 is a solvent accessible residue located on the protein surface, and replacement of this residue with histidine changes the charge and polarity of this region. It has been suggested that this may cause aberrant incorporation of copper or trafficking of Cp (Hofmann et al., 2007). Our results indicate that aberrant incorporation of copper because of impairment of the interaction with ATP7B may be the best explanation; reconstitution with Cu(I)-GSH would lead to a protein that contains copper but is inactive.

A final remark must be made on those mutants that appear to be partially (F198S and A331D) or fully (I9F, Q146E, W264S, G606E, and G876A) functional in our system. This finding implies that the protein retains (at least partially) ferroxidase activity. It is worth noting that aceruloplasminemia is a late onset pathology, and these mutations were identified in heterozygous patients with mild neurologic symptoms (I9F and G876A) or also suffering from a multiple system atrophy (G606E) (Daimon et al., 2000, Yomono et al., 2003).

Q146E is found in compound heterozygosity with a Cp truncated at residue 983 (Bosio et al., 2002), and W264S is homozygous (Shang et al., 2006), with both patients exhibiting neurologic symptoms. The position of these mutations in the structure of Cp suggests that the protein can retain ferroxidase activity. This assumption is supported by the presence of holo-Cp in the supernatants of transfected cells shown in Fig. 1D. Recombinant Cp-GPI I9F was found to be prevalently retained in the ER (Kono et al., 2006); however, it is reasonable to assume that the fraction of protein that escapes can complete its maturation generating holo-Cp.

Cp mutants F198S and A331D show partial complementation. These are two homozygous mutations not associated with neurologic deficits, possibly because of the age of the patients (Mariani et al., 2004). The impact of these two substitutions on the structure of Cp appears to be more serious; Phe-198 is located in the same hydrophobic pocket where Pro-177 is found, suggesting a folding defect; Ala-331 is close to the type 1 copper site of domain 2, and substitution with a negatively charged amino acid could cause defective copper incorporation. Actually, replacement of Phe-198 or Ala-331 with other residues (F198Y/F198T and A331V/A331N) produced the same results in the functional complementation assay as the variants detected in the patients (data not shown), strongly implying that it is the position of the mutation in the Cp structure that is critical, irrespective of the substituted amino acid.

It should be reminded that in our model system the missense mutants (and Fpn-GFP) are over-expressed under control of the strong cytomegalovirus promoter; therefore, it is possible that even if the specific ferroxidase activity of the mutant protein is low, the amount of recombinant protein produced is sufficient to guarantee ‘survival’ of Fpn at the plasma membrane. Clearly, it would be necessary to measure the specific activity of these mutants to verify the full impact of the amino acid substitution on Cp. Preliminary data obtained on the missense mutants expressed in yeast suggest that specific activity is lower than that of the WT and that a correlation between functional complementation in mammalian cells and oxidase activity exists (data not shown).

In conclusion, our results show for the first time that some forms of aceruloplasminemia are in principle reversible, as the responsible missense mutation leads to a protein that is inactive because of lack of copper, yet has the potential of acquiring it, with noteworthy consequences on possible therapeutic strategies.

REFERENCES

Abboud S, Haile DJ. (2000) *J. Biol. Chem.* **275**, 19906–19912

Aldred AR, Grimes A, Schreiber G, Mercer JF. (1987) *J. Biol. Chem.* **262**, 2875–2878

Andrews NC. (1999) *N. Engl. J. Med.* **341**, 1986–1995

Andrews NC. (2000) *Nat. Rev. Genet.* **1**, 208–217

Angelova-Gateva P. (1980) *Agressologie* **21**, 27–30

Askwith C, Eide D, Van Ho A, Bernard PS, Li L et al. (1994) *Cell* **76**, 403–410

Bacsi A, Woodberry M, Widger W, Papaconstantinou J, Mitra S, Peterson JW, Boldogh I. (2006) *Mitochondrion* **6**, 235–244

Bento I, Peixoto C, Zaitsev VN, Lindley PF. (2007) *Acta Cryst.* **D63**, 240–248

Bento I, Martins LO, Lopes GG, Carrondo MA, Lindley PF. (2005) *Dalton Trans.* **21**, 3507–3513

Bielli P, Bellenchi GC, Calabrese L. (2001) *J. Biol. Chem.* **276**, 2678–2685

Boldogh I, Roy G, Lee MS, Bacsi A, Hazra TK, Bhakat KK, Das GC, Mitra S. (2003) *Toxicology* **193**, 137–152

Bosio S, De Gobbi M, Roetto A, Zecchina G, Leonardo E, Rizzetto M, Lucetti C, Petrozzi L, Bonuccelli U, Camaschella C. (2002) *Blood* **100**, 2246-2248

Bradbury M. (1997) *J. Neurochem*. **69**, 443–454

Brock J. (1995) *Immunol. Today* **9**, 417–419

Burdo JR, Menzies SL, Simpson IA, Garrick LM, Garrick MD, Dolan KG, Haile

DJ, Beard JL, Connor JR. (2001) *J. Neurosci. Res.* **66**, 1198–1207

Cairo G, Pietrangelo, A. (2000) *Biochem. J.* **352**, 241–250

Calabrese L, Carbonaro M, Musci G. (1989) *J. Biol. Chem.* **264**, 6183–6187

Chen L, Dentchev T, Wong R, Hahn P, Wen R, Bennett J, Dunaief JL. (2003) *Mol. Vis.* **9**, 151-158

Church WR, Jernigan RL, Toole J, Hewick RM, Knopf J, et al. (1984) *Proc. Nat. Acad. Sci. USA* **81**, 6934–6937

Copp AJ, Estibeiro JP, Brook FA, Downs KM. (1992) *Dev. Biol.* **153**, 312–323

Craven CM, Alexander J, Eldridge M, Kushner JP, Bernstein S, et al. (1987) *Proc. Natl. Acad. Sci. USA* **84**, 3457–3461

Daimon M, Yamatani K, Igarashi M, Fukase N, Kawanami T, et al. (1995) *Biochem. Biophys. Res. Commun.* **208**, 1028–1035

Daimon M, Susa S, Ohizumi T, Moriai S, Kawanami T, Hirata A, Yamaguchi H, Ohnuma H, Igarashi M, Kato T. (2000) *Tohoku J. Exp. Med.* **191**, 119-125

De Domenico I, Lo E, Ward DM, Kaplan J. (2009) *Proc. Natl. Acad. Sci. USA* **106**, 3800-3805

De Domenico I, McVey Ward D, Bonaccorsi di Patti MC, Jeong SY, David S, Musci G, Kaplan J. (2007) *EMBO J.* **26,** 2823-2831

De Domenico, I., Nemeth, E., Nelson, J.M., Phillips, J.D., Ajioka, R.S., Kay, M.S., Kushner, J.P., Ganz, T., Ward, D.M., Kaplan, J. (2008) *Cell Metab.* **8**, 146-156

De Domenico I, Ward DM, Nemeth E, Vaughn MB, Musci G, Ganz T, Kaplan, J. (2005) *Proc. Natl. Acad. Sci. USA* **102**, 8955–8960

Donovan A, Lima CA, Pinkus JL, et al. (2005) *Cell Metabolism* **1**, 191–200

Ducros V, Brzozowski AM, Wilson KS, Ostergaard P, Schneider P, Svendson A, Davies GJ. (2001) *Acta Cryst.* **D57**, 333–336

El Meskini R, Culotta VC, Mains RE, Eipper BA. (2003) *J. Biol. Chem.* **278**, 12278–12284

Faucheux BA, Nillesse N, Damier P. et al. (1995) *Proc. Natl Acad. Sci. USA* **92**, 9603–9607

Fillebeen C, Descamps L, Dehouck M-P, Fenart L, Benaissa M, Spik G, Cecchelli R, Pierce A. (1999) *J. Biol. Chem*. **274**, 7011–7017

Fleming R, Gitlin JD. (1990) *J. Biol. Chem*. **265**, 7701–7707

Fortna RR, Watson HA, Nyquist SE. (1999) *Biol. Reprod*. **61**, 1042–1049

Fujita Y, Okamoto K, Sakurai A, Gonatas NK, Hirano A. (2000) *J. Neurol. Sci.* **174**, 137–140

Ganz T, Nemeth E (2006) *Am. J. Physiol. Gastrointest. Liver Physiol.* **290**, G199–G203

Garavaglia S, Cambria MT, Miglio M, Ragusa S, Iacobazzi V, Palmieri F, D'Ambrosio C, Scaloni A, Rizzi M. (2004) *J. Mol. Biol*. **342**, 1519–1531

Gaxiola RA, Yuan DS, Klausner RD, Fink GR. (1998) *Proc. Natl. Acad. Sci. USA* **95**, 4046–4050

Genty B, Briantais JM, Baker NR. (1989) *Biochim. Biophys. Acta* **990**, 87–92

Gitlin JD. (1988) *J. Biol. Chem.* **63**, 6281–6287

Gonatas NK, Stieber A, Gonatas JO. (2006) *J. Neurol. Sci* **246**, 21–30

Gunshin H, Mackenzie B, Berger UV, Gunshin Y, Romero MF, Boron WF, Nussberger S, Gollan JL, Hediger MA. (1997) *Nature* **388**, 482–488

Hamza I, Faisst A, Prohaska J, Chen J, Gruss P, et al. (2001) *Proc. Natl. Acad. Sci. USA* **98**, 6848–6852

Hansen TM, Nielsen H, Bernth N, Moos T. (1999) *Mol. Brain Res*. **65**, 186–197

Harris ZL, Takahashi Y, Miyajima H, Serizawa M, MacGillivray RT. (1995) *Proc. Natl. Acad. Sci. USA* **92**, 2539–2543

Harris ZL, Durley AP, Man TK, Gitlin JD. (1999) *Proc. Natl. Acad. Sci. USA* **96**, 10812-10817

Hellman NE, Gitlin JD. (2002) *Annu. Rev. Nutr*. **22**, 439-458

Hellman NE, Kono S, Miyajima H, Gitlin JD. (2002) *J. Biol. Chem.* **277**, 1375–1380

Hellman NE, Kono S, Mancini GM, Hoogeboom AJ, De Jong GJ, Gitlin JD. (2002) *J. Biol. Chem.* **277**, 46632-46638

Hofmann WP, Welsch C, Takahashi Y, Miyajima H, Mihm U, Krick C, Zeuzem S, Sarrazin C. (2007) *Scand. J. Gastroenterol.* **42**, 1088-1094

Holmberg CG, Laurell CB. (1948) *Acta Chem. Scand*. **2**, 550–556

Holtzman NA, Gaumnitz BM. (1970) *J. Biol. Chem*. **245**, 2354–2358

Hsi G, Cullen LM, Macintyre G, Chen MM, Glerum DM, Cox DW. (2008) *Hum. Mutat*. **29**, 491–501

Hung IH, Suzuki M, Yamaguchi Y, Yuan DS, Klausner RD, Gitlin JD. (1997) *J. Biol. Chem.* **272**, 21461–21466

Jefferies WA, Brandon MR, Hunt SV, Williams AF, Gatter KC, Mason DY. (1984) *Nature* **312**, 162–163

Jeong SY, David S. (2006) *J. Neurosci*. **26**, 9810–9819

Kawabata H, Yang R, Hirama T, Vuong PT, Kawano S, Gombart AF, Koeffler HP. (1999) *J. Biol. Chem*. **274**, 20826–20832

Klomp LW, Farhangrazi ZS, Dugan LL, Gitlin JD. (1996) *J. Clin. Invest*. **98**, 207–215

Kono S, Miyajima H. (2006) *Biol. Res*. **39**, 15–23

Kono S, Suzuki H, Oda T, Miyajima H, Takahashi Y, Shirakawa K, Ishikawa K, Kitagawa M. (2006) *Neuromolecular Med*. **8**, 361–374

Kono S, Suzuki H, Oda T, Shirakawa K, Takahashi Y, Kitagawa M, Miyajima H. (2007) *J. Hepatol*. **47**, 844–850

Koschinsky ML, Chow BK-C, Schwartz J, Hamerton JL, MacGillivray RTA. (1987) *Biochemistry* **26**, 7760–7767

Koschinsky ML, Funk WD, VanOost BA, MacGillivray RT. (1986) *Proc. Natl. Acad. Sci. USA* **83**, 5086–5090

Kuhn J, Miyajima H, Takahashi Y, Kunath B, Hartmann-Klosterkoetter U, Cooper-Mahkorn D, Schaefer M, Bewermeyer H. (2005) *J. Neurol*. **252**, 111–113

Larin D, Mekios C, Das K, Ross B, Yang AS, et al. (1999) *J. Biol. Chem.* **274**, 28497–28504

Lee GR, Nacht S, Lukens JN, Cartwright GE. (1968) *J. Clin. Invest.* **47**, 2058–2069

Leveugle B, Spik G, Perl DP, Bouras C, Fillit HM, Hof PR. (1994) *Brain Res*. **650**, 20–31

Levy JE, Jin O, Fujiwara Y, Kuo F, Andrews NC. (1999) *Nat. Genet.* **21**, 396–399.

Lindley PF, Card G, Zaitseva I, Zaitsev V, Reinhammar B, Selin-Lindgren E, Yoshida K. (1997) *J. Biol. Inorg. Chem*. **2**, 454–463

Liu XB, Yang F, Haile DJ (2005) *Blood Cells Mol. Dis.* **35**, 33-46

Logan JL, Harveyson KB, Wisdom GB, Hughes AE, Archibold GP. (1994) *Q. J. Med*. **87**, 663–670

Loudianos G, Gitlin JD. (2000) *Semin. Liver Dis.* **20**, 353–364

Lutsenko S, Barnes NL, Bartee MY, Dmitriev OY. (2007) *Physiol. Rev.* **87**, 1011-1046

Machonkin TE, Quintanar L, Palmer AE, Hassett R, Severance S, et al. (2001) *J. Am. Chem. Soc.* **123**, 5507–5517

Machonkin, TE, Solomon EI. (2000) *J. Am. Chem. Soc*. **122**, 12547–12560

Mariani R, Arosio C, Pelucchi S, Grisoli M, Piga A, Trombini P, Piperno A. (2004) *Gut* **53**, 756-758

McKie AT, Marciani P, Rolfs A. et al. (2000) *Mol. Cell* **5**, 299–309

Messerschmidt A, Ladenstein R, Huber R, Bolognesi M, Avigliano L, Petruzzelli R, Rossi A, Finazzi Agro A. (1992) *J. Mol. Biol*. **224**, 179–205

Messerschmidt A, Rossi A, Ladenstein R, Huber R, Bolognesi M, et al. (1989) *J. Mol. Biol.* **206**, 513–529

Mittal B, Doroudchi MM, Jeong SY, Patel BN, David S. (2003) *Glia* **41**, 337-346

Moos T, Morgan EH. (1998a) *Brain Res*. **790**, 115–128

Moos T, Morgan EH. (1998b) *J. Neurosci. Res*. **54**, 486–494

Moos T, Morgan EH. (2004) *J. Neurochem*. **88**, 233–245

Moos T, Rosengren Nielsen T. (2006) *Semin. Pediatr. Neurol.* **13**, 49–57

Moos T, Rosengren Nielsen T, Skjørringe T, Morgan EH. (2007) *J. Neurochem.* **103**, 1730–1740

Morgan E. (1981) *Mol. Aspects Med.* **4**, 1–123

Musci G, Di Marco S, Bellenchi GC, Calabrese L. (1996) *J. Biol. Chem.* **271**, 1972-1978

Nakagomi S, Barsoum MJ, Bossy-Wetzel E, Sütterlin C, Malhotra V, Lipton SA. (2008) *Neurobiol. Dis.* **29**, 221-231

Nemeth E, Tuttle MS, Powelson J, Vaughn MB, Donovan A, Ward DM, Ganz T, Kaplan J (2004) *Science* **306**, 2090–2093

Nemeth E, Ganz T. (2006) *Annu. Rev. Nutr*. **26**, 323-342

Osaki S, Johnson D, Frieden E. (1966) *J. Biol. Chem.* **241**, 2746–2757

Osaki S, Johnson DA, Frieden E. (1971) *J. Biol. Chem.* **246**, 3018–3023

Park CH, Valore EV, Waring AJ, Ganz T. (2001) *J. Biol. Chem.* **276**, 7806–7810

Patel BN, David S. (1997) *J. Biol. Chem.* **272**, 20185–20190

Patel BN, Dunn RJ, David S. (2000) *J. Biol. Chem.* **275**, 4305-4310

Pietrangelo A. (2006) *Biochim. Biophys. Acta* **1763**, 700–710

Piontek K, Antorini M, Choinowski T. (2002) *J. Biol. Chem*. **277**, 37663–37669

Rae TD, Schmidt PJ, Pufahl RA, Culotta VC, O'Halloran TV. (1999) *Science* **284**, 805–808

Rice AE, Mendez MJ, Hokanson CA, Rees DC, Bjorkman PJ. (2009) J. *Mol. Biol*. **386**, 717-732

Robbins E, Gonatas NK. (1964) *J. Cell Biol*. **21**, 429–463

Roeser HP, Lee GR, Nacht S, Cartwright GE. (1970) *J. Clin. Invest.* **49**, 2408-2417

Roetto A, Papanikolaou G, Politou M, et al. (2003) *Nature Genetics* **33**, 21–22

Rosenzweig AC. (2000) *Acc. Chem. Res.* **34**, 119–128

Roy CN, Mak HH, Akpan I, Losyev G, Zurakowski D, Andrews NC. (2007) *Blood* **109**, 4038–4044

Sato M, Gitlin JD. (1991) *J. Biol. Chem.* **266**, 5128–5134

Shang HF, Jiang XF, Burgunder JM, Chen Q, Zhou D. (2006) *Mov. Disord.* **21**, 2217-2220

Scheinberg IH, Gitlin D. (1952) *Science* **116**, 484–489

Schosinsky KH, Lehmann HP, and Beeler MF (1974) *Clin. Chem.* **20**, 1556-1563

Sears IB, O'Connor J, Rossanese OW, Glick BS. (1998) *Yeast* **14**, 783–790

Siebert PD, Huang BC. (1997) *Proc. Natl. Acad. Sci. USA* **94**, 2198-2203

Solomon EI, Sundaram UM and Machonkin TE (1996) *Chem. Rev.* **96**, 2563-2605

Stearman R, Yuan DS, Yamaguchi-Iwa Y, Klausner RD, Dancis A. (1996) *Science* **271**, 1552–1557

Stieber A, Gonatas JO, Moore JS, Bantly A, Yim HS, Yim MB, Gonatas NK. (2004) *J. Neurol. Sci*. **219**, 45–53

Sutterlin C, Hsu P, Mallabiabarrena A, Malhotra V. (2002) *Cell* **109**, 359–369

Takahashi N, Ortel TL, Putnam FW. (1984) *Proc. Natl. Acad. Sci. USA* **81**, 390–394

Taylor EM, Morgan EH. (1990) *Dev. Brain Res*.**55**, 35–42

Terada K, Kawarada Y, Miura N, Yasui O, Koyama K, et al. (1995) *Biochim. Biophys. Acta* **1270**, 58–62

Terent A, Hallgren R, Venge P, Bergstrom K. (1981) *Stroke* **12**, 40–46

Tulpule K, Robinson SR, Bishop GM, Dringen R. (2010) *J. Neurosci. Res.* **88**, 563–571

Vulpe CD, Kuo YM, Murphy TL, Cowley L, Askwith C, et al. (1999) *Nat. Genet.* **21,** 195–199

Wang T, Weinman SA. (2004) *Gastroenterology* **126**, 1157-1166

Warren G. (1993) *Annu. Rev. Biochem.* **62**, 323–348

Wessling-Resnick M. (2006) *Am. J. Physiol. Gastrointest. Liver Physiol*. **290**, G1–G6

Wu LJ, Leenders AG, Cooperman S, Meyron-Holtz E, Smith S, Land W, Tsai RY, Berger UV, Sheng ZH, Rouault TA. (2004) *Brain Res*. **1001**, 108–117

Yang F, Naylor SL, Lum JB, Cutshaw S, McCombs JL, et al. (1986) *Proc. Natl. Acad. Sci. USA* **83,** 3257–3261

Yang FM, Friedrichs WE, Cupples RL, Bonifacio MJ, Sanford JA, et al. (1990) *J. Biol. Chem.* **26**, 10780–10785

Yomono H, Kurisaki H, Murayama S, Hebisawa A, Miyajima H, Takahashi Y. (2003) *Rinsho Shinkeigaku* **43**, 398-402

Yoshida K, Furihata K, Takeda S, Nakamura A, Yamamoto K, et al. (1995) *Nat. Genet.* **9**, 267–272

Yuan DS, Stearman R, Dancis A, Dunn T, Beeler T, Klausner RD. (1995) *Proc. Natl. Acad. Sci. USA* **92**, 2632–2636

Zhang L, Sheng R, Qin Z. (2009) *Acta Biochim. Biophys. Sin.* **41**, 437-445

Zaitseva I, Zaitsev V, Card G, Moshkov K, Bax B, et al. (1996) *J. Biol. Inorg. Chem.* **1**, 15–23

PUBLICATIONS

Maio N, Polticelli F, De Francesco G, Rizzo G, Bonaccorsi di Patti MC, Musci G. (2010) Role of external loops of human ceruloplasmin in copper loading by ATP7B and Ccc2p. *J. Biol. Chem.* **285**, 20507-20513.

Bonaccorsi di Patti MC, Maio N, Rizzo G, De Francesco G, Persichini T, Colasanti M, Polticelli F, Musci G. (2009) Dominant mutants of ceruloplasmin impair the copper loading machinery in aceruloplasminemia. *J. Biol. Chem.* **284**, 4545-4554.